Reliability Analysis of Phaedrus

Yoichi Watanabe

January 1987

UWFDM-716

FUSION TECHNOLOGY INSTITUTE

UNIVERSITY OF WISCONSIN

MADISON WISCONSIN

Reliability Analysis of Phaedrus

Yoichi Watanabe

Fusion Technology Institute
University of Wisconsin
1500 Engineering Drive
Madison, WI 53706

http://fti.neep.wisc.edu

January 1987

UWFDM-716

RELIABILITY ANALYSIS OF PHAEDRUS

Yoichi Watanabe

Fusion Technology Institute
1500 Johnson Drive
University of Wisconsin-Madison
Madison, Wisconsin 53706

January 1987

UWFDM-716

TABLE OF CONTENTS

1. INTRODUCTION

Availability is defined as the length of uptime (time during which a system is working properly) divided by the uptime plus the length of downtime (time during which a system is not working) and it is one of the most important measures to indicate the quality of system performance.

The availability in fusion technology is and will be a major concern for experimental devices, engineering test facilities (ETFs), and commercial power plants. The availability of a commercial power plant affects the cost of electricity (COE); in fact, COE is approximately inversely proportional to the availability [1]. Engineering test facilities being planned for the next decade will be strongly affected by the availability since the availability determines the length of operation required to collect sufficient data for the next step [2]. The availability of scientific experimental devices has attracted less attention than other systems. Present fusion experimental devices such as TFTR, JET, and JT-60 are very large, complex, and expensive from both the construction and operation points of view. Hence, some work with regard to availability has been initiated. Studies are being performed at the entire system level [3-5] and at the subsystem/component levels [6-13]. The efforts can be classified as follows:

(1) Identify weak components, which mostly contribute to unavailability of the system, by testing and recording the performance. Then, try to improve the quality of those components.

(2) Extrapolate/predict the reliability of components for future devices by observing the performance of existing systems.

(3) Collect reliability data of systems for future uses.

In order to predict the availability of a system on a drawing board, we need models of system structure, operation, and failure/repair and data on component reliability and maintenance. The current small efforts can be useful in obtaining the data [14], although the efforts should be more organized locally and internationally. We have developed two computer simulation programs, AVSYS and PROPA, which are capable of modeling sophisticated operations [15,16], and a symbolic analysis program REDFOR [17] for availability analysis. Computerized data management programs FUSEDATA [18] and an adaptation of CREDO [19] have been developed. FUSEDATA is aimed at fusion reactor and subsystem designs. Meanwhile, CREDO is designed for fast reactor data collection and has been adapted for use in fusion at the Tritium Systems Test Assembly at the Los Alamos National Laboratory.

To collect more data, examine the current modeling capability, and eventually fill out FUSEDATA, we are proposing to perform analyses of existing fusion engineering systems. The present report describes an initial result of the work being performed for a tandem mirror experimental device Phaedrus at the University of Wisconsin-Madison. The objectives of this study are:

(a) to create system models of Phaedrus,

(b) to modify CREDO for data collection at Phaedrus,

(c) to analyze Phaedrus reliability by using currently available data and make some suggestions for reliability/productivity improvement.

Following this introduction, Section 2 describes the system and models created. Section 3 describes the data collected by interviewing the laboratory personnel and adaptation of CREDO to the Phaedrus facility. Section 4 describes initial analyses. In the final section some conclusions are made and future research areas are proposed.

2. MODEL

2.1 Phaedrus Tandem Mirror

The tandem mirror Phaedrus was designed to test RF heating techniques for auxiliary heating and low energy neutral beam refueling and investigate confinement properties of tandem mirrors [20]. Recently the experiments have been focused on RF techniques at the ion cyclotron and electron cyclotron ranges of frequencies. The RF techniques are being used for not only plasma heating but also fueling, electric potential modification, MHD stability, and startup [21,22]. The device is about 10 m long and located in the basement of the Engineering Research Building (ERB) at the University of Wisconsin-Madison campus. It is a multimillion dollar machine. Experiments are performed by a number of research staff and students under the leadership of Professor N. Hershkowitz of the Nuclear Engineering and Engineering Physics Department.

Large projects such as the TFTR experiment cost a hundred million dollars for construction and millions of dollars for annual operation. They employ hundreds of scientists and engineers. The devices are designed and built by contracted companies under detailed specification. There are a number of quality assurance personnel and maintenance engineers who take care of day-to-day operation. On the other hand, medium size experiments such as Phaedrus, which cost millions of dollars for equipment and hundreds of thousands of dollars for annual operation and employ tens of research staff, do not usually have people specializing in quality control and maintenance. Experimental setups are frequently modified by individual decisions. Researchers are experimentalists, maintenance men, and equipment designers and manufacturers, simultaneously.

2.2 System Model

A hierarchical approach is chosen to construct a system model of Phaedrus. The entire Phaedrus device is analyzed. The system is decomposed into the subsystems: Normal Magnets System (MC), Distilled Water Supply System (WS), Vacuum System (VS), ICRF System (RF), Plasma Production System (PP), Diagnostics System (DS), Data Acquisition and Computer System (DC), and Operators/Scientists (OP). The systems tree is given in Fig. 2-1.

2.2.1 Normal Magnets System (MC)

The MC system is used to create a magnetic field ranging from 500 gauss at the central cell region up to 5 kG at the end cells. A number of solenoid coils and Ioffe coils are located along the axis of the device as illustrated in Fig. 2-2. There is a low power source and a high power source. A transformer specific to the Phaedrus device is located at the Randall Station of the Madison Gas and Electric company (MGE) and supplies power to the high power source. The low power is provided directly from the ERB power supply. The high power source is used for high current coils at the end plugs. The rest of the coils are powered by the low power source. The slow timer is used to initiate a pulse with a length of 5 seconds. The SCR switches and coils are cooled by distilled water. Figure 2-3 shows the functional block diagram of this system. Table 2-1 gives a listing of components and ID names. A systems tree is constructed and given in Fig. 2-4.

2.2.2 Distilled Water Supply System (WS)

Hard water damages devices being cooled. Hence a distillation system is installed to remove calcium, magnesium, and other impurities from city water [23]. A functional block diagram of the WS system is given in Fig. 2-5. Dis-

Table 2-1. Components in MC

Component	ID
Fuses #1, 2	FS#
Transformer (0.75 MW)	TR1
Transformer (3.5 MW)	TR2
Transformer (2.5 MW)	TR3
Transformer (1 MW)	TR4
Circuit breaker #1, 2, 3	CB#
Power source ERB	ERB
Power source MGE Randall station	MGE
Power supply (600 KW) #1 to 4	PS#
Power supply (3 MW) #1 to 3	PH#
Slow timer	TM#
SCR #1 to 6	SC#
Central cell coil	CCC
Saddle coil A	SCA
Mirror solenoid coil	MSC
Choke coil	CHC
Saddle coil B	SCB
Coil	COL
Ioffe bar #1, 2	IF#

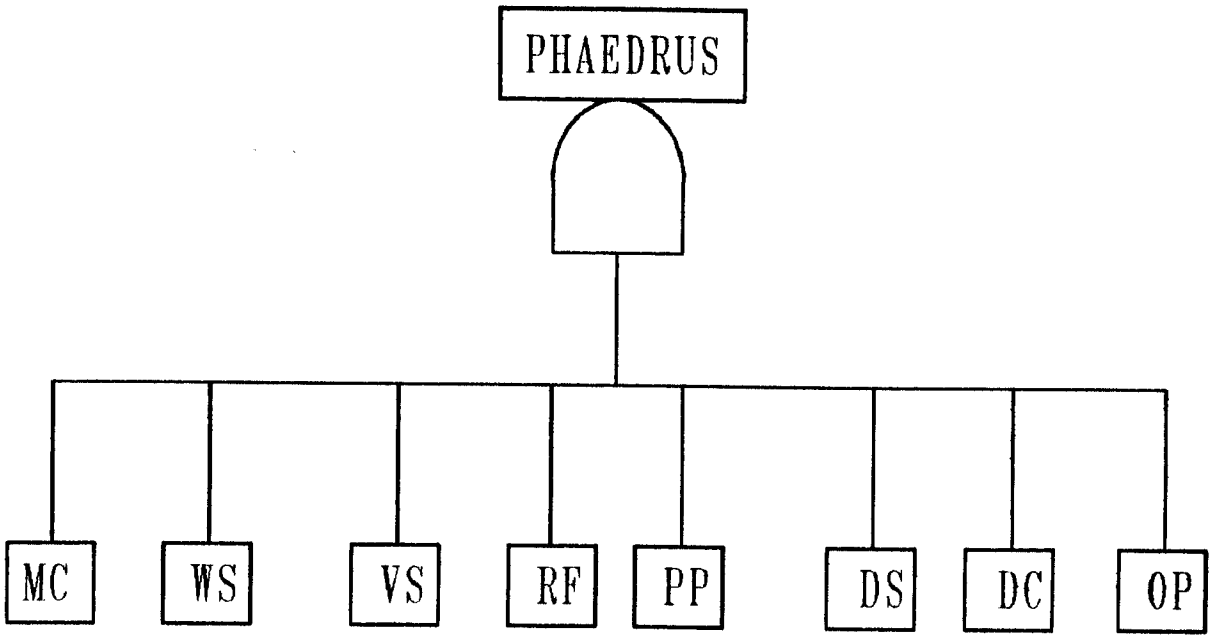

Fig. 2-1. Systems tree of Phaedrus.

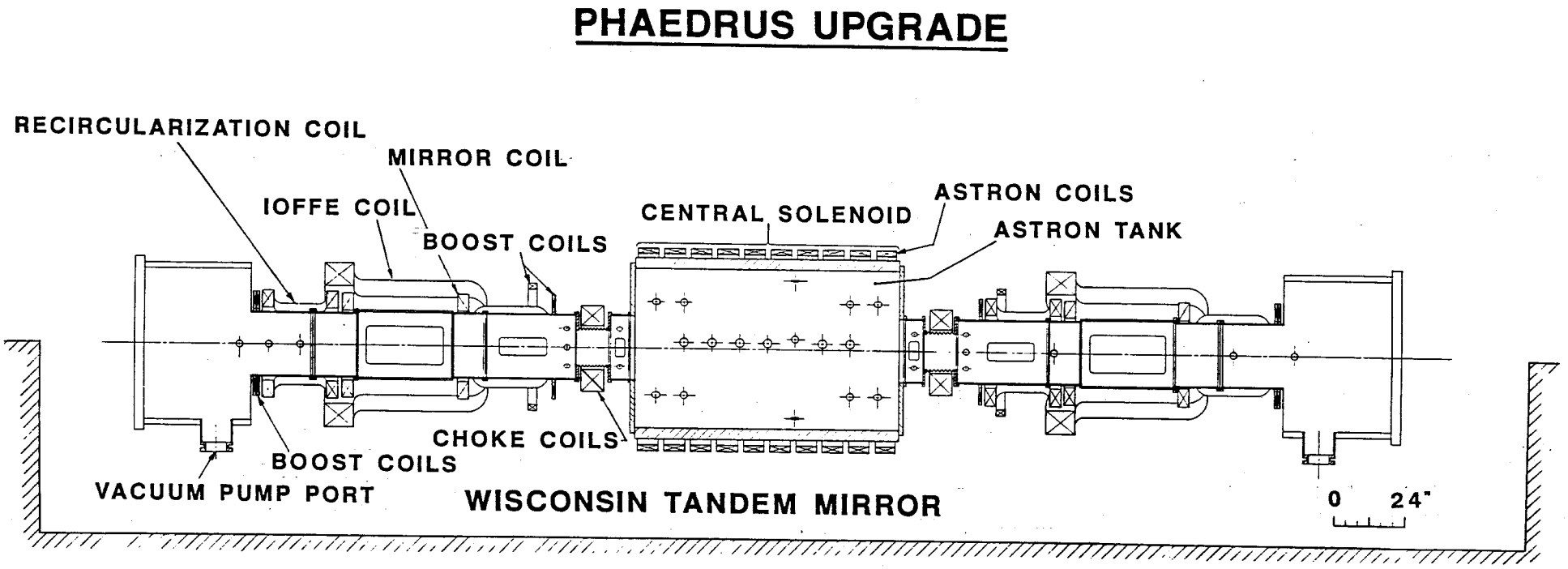

Fig. 2-2. Schematic of coil locations.

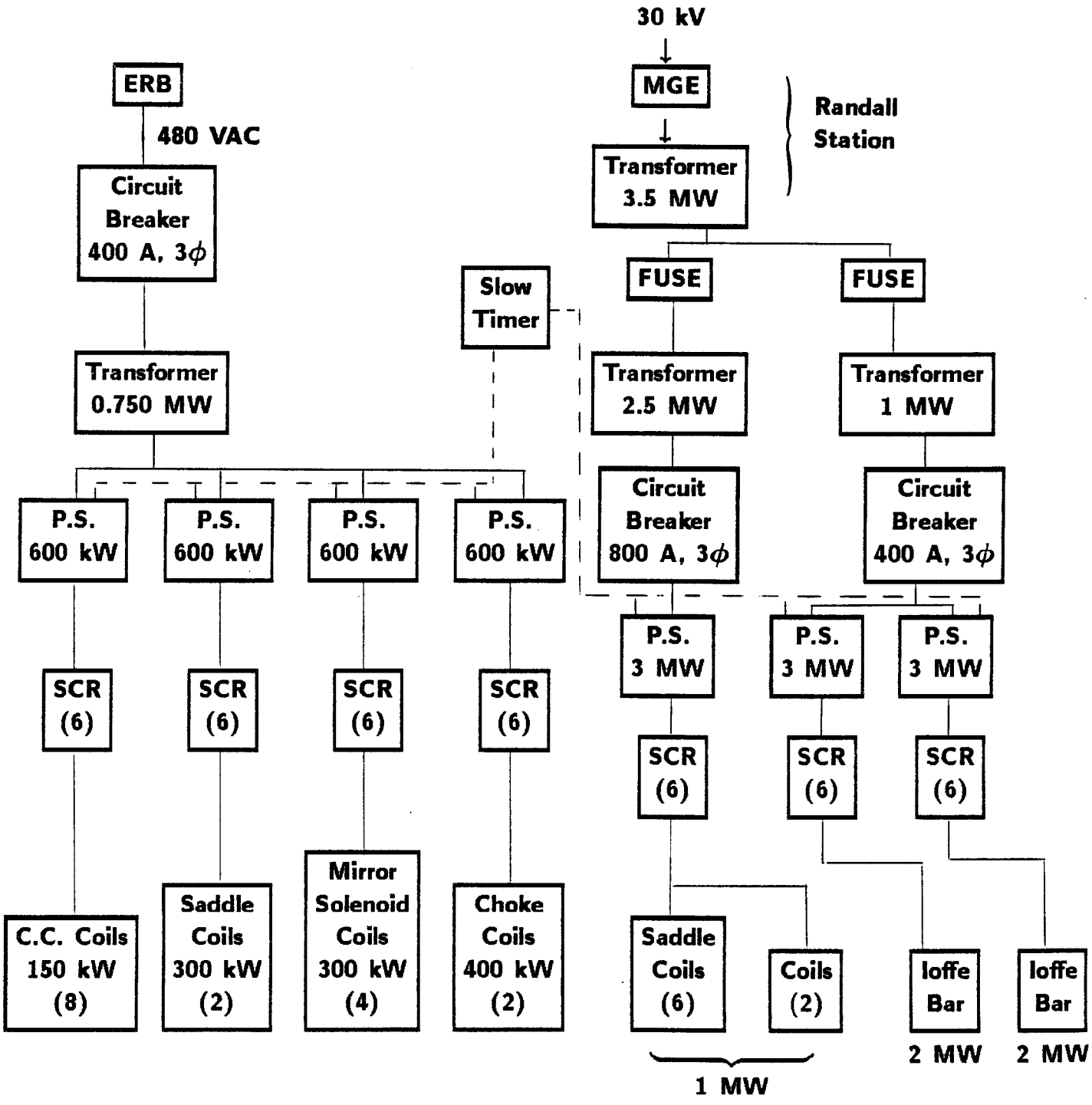

Fig. 2-3. Functional block diagram of the Normal Magnets System.

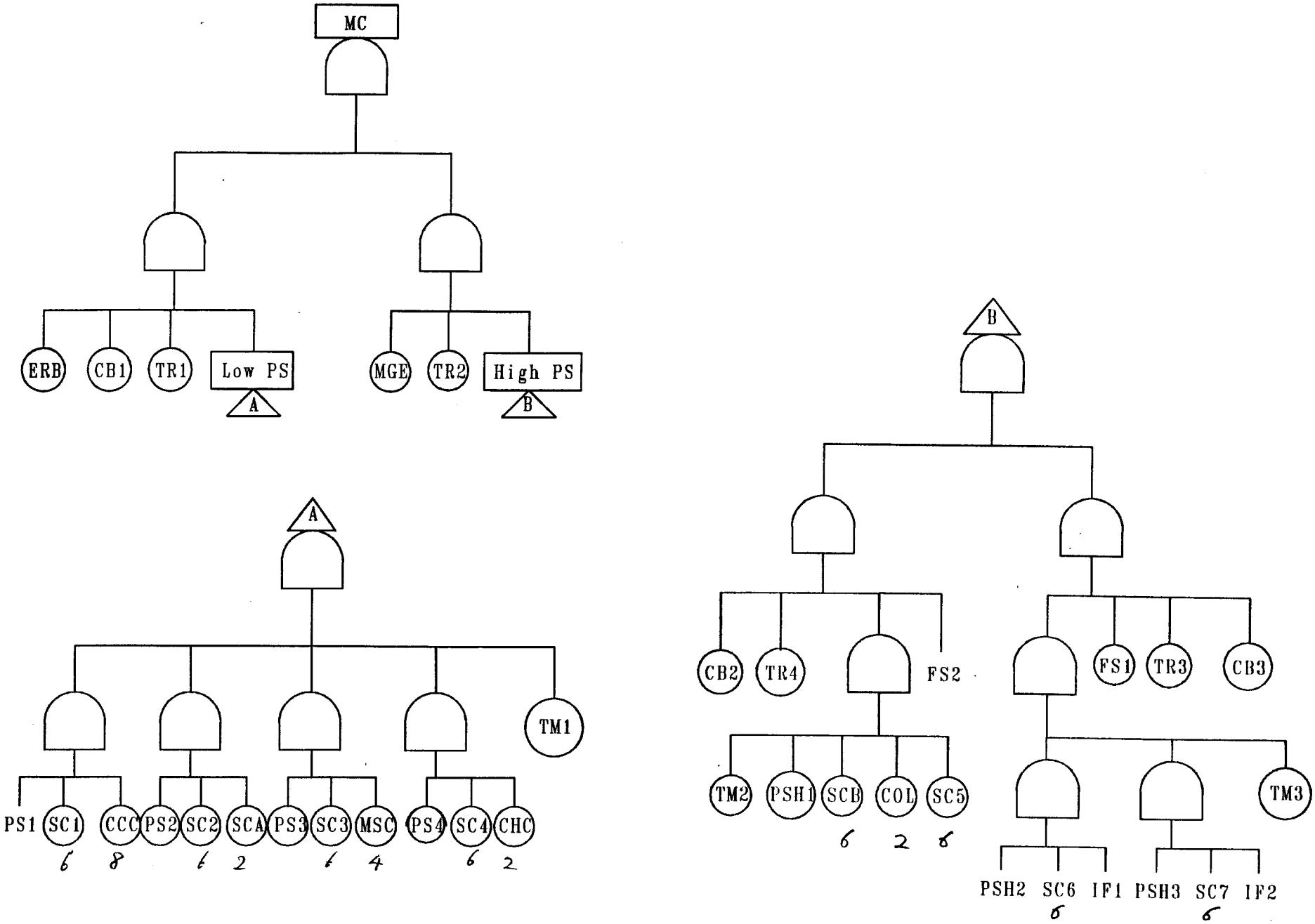

Fig. 2-4. Systems tree of Normal Magnets System.

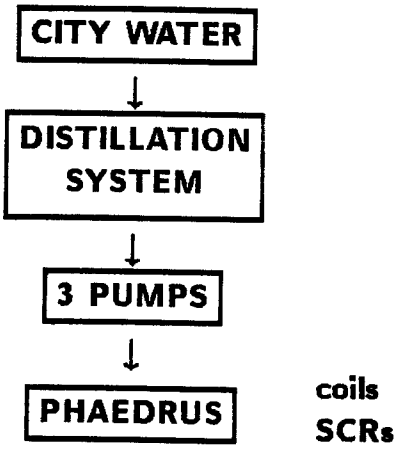

Fig. 2-5. Functional block diagram of Distilled Water Supply System.

tilled water is used to cool normal coils, SCRs, cryopumps, turbopumps, amplifiers and oscillator tubes in RF systems. A listing of components is given in Table 2-2. Figure 2-6 shows a systems tree.

2.2.3 Vacuum System (VS)

There are five roughing pumps, two cryopumps, two turbopumps, and one titanium sublimator. The cryopumps and turbopumps are water-cooled. The 50 ℓ/s roughing pump is used to pump the vacuum vessel first. Then cryopumps and turbopumps are turned on until a vacuum of 10^{-6} torr is reached. Finally the titanium sublimator is switched on to obtain a vacuum of 10^{-7} to 10^{-8} torr. For normal operation the turbopumps and the titanium sublimators are required. The turbopumps are operated 24 hours a day. One of the turbopumps is redundant. There are one manual and four pneumatic valves. The pneumatic valves are opened/closed by the controller based on the measurement of vacuum by the ion gauge.

A functional diagram and a listing of components are given in Fig. 2-7 and Table 2-3, respectively. Figure 2-8 shows the systems tree.

2.2.4 ICRF System (RF)

A 300 kW and a 200 kW ICRF system that generate 1.3 MHz RF waves are installed at the central cell. Four 100 kW ICRF systems that generate 5 MHz RF waves are installed at the end cells (two systems at each end). The locations of antennas are illustrated in Fig. 2-9. The functional diagram is given in Fig. 2-10. The 300 kW ICRF system (CC#1) has three stages of amplifiers: waves of mW power generated by the synthesizer are amplified to 40 W, 2 kW, and 300 kW by the amplifiers, successively. The second and final amplifiers are powered by their own capacitor banks. The antenna is installed inside the

Table 2-2. Components of WS

Component	ID
City water supply	CWS
Distillation system	DIS
Water pumps	PMP
Pipes	PIP
Valves	VLV

Table 2-3. Components in VS System

Components	ID
Vacuum vessel	VCV
Roughing pump (50 ℓ/s)	RP5
Roughing pump #1 to 4	RP#
Cryopump #1, 2	CP#
Turbopump (450 ℓ/s) #1, 2	TP#
Manual gate valve	MGV
Pneumatic gate valve #1 to 4	NV#
Titanium sublimator	TSB
Ion gauge	IOG
Controller	CTL
Water supply #1 to 4	WT#

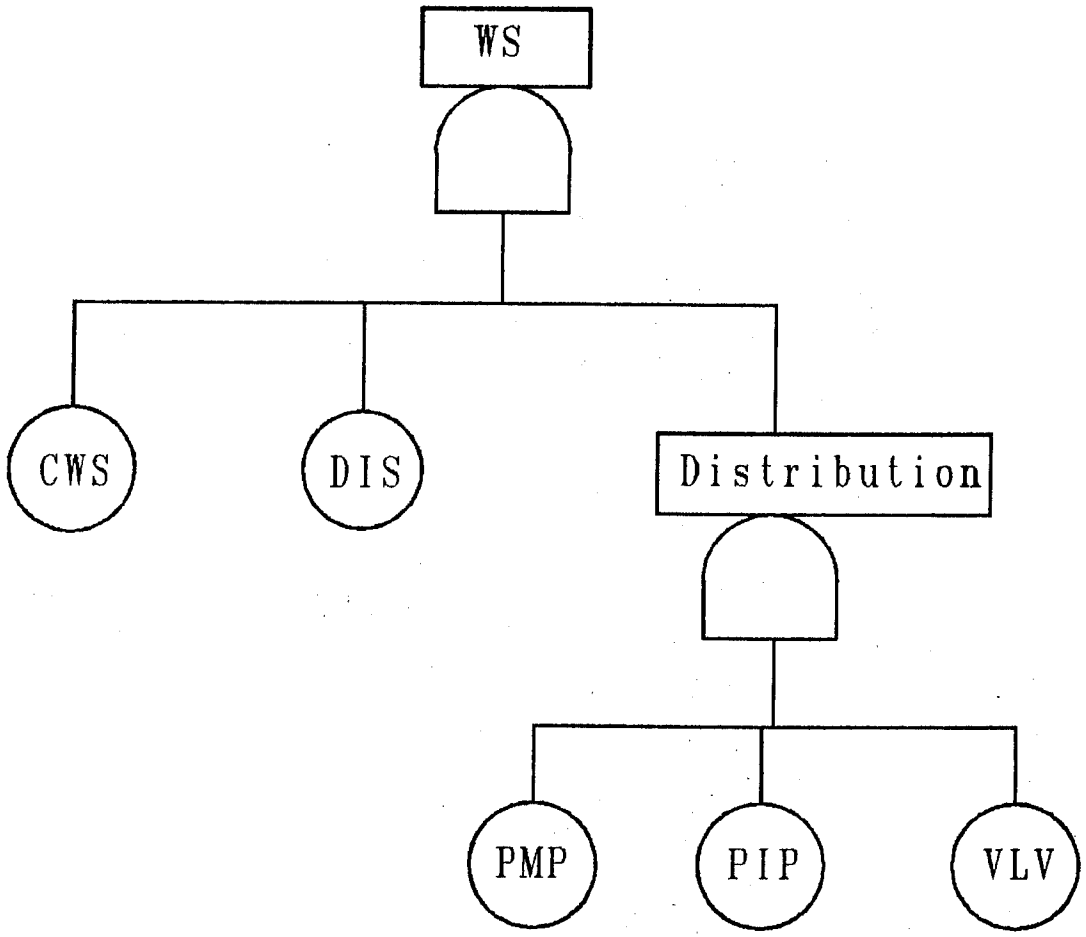

Fig. 2-6. Systems tree of Distilled Water Supply System.

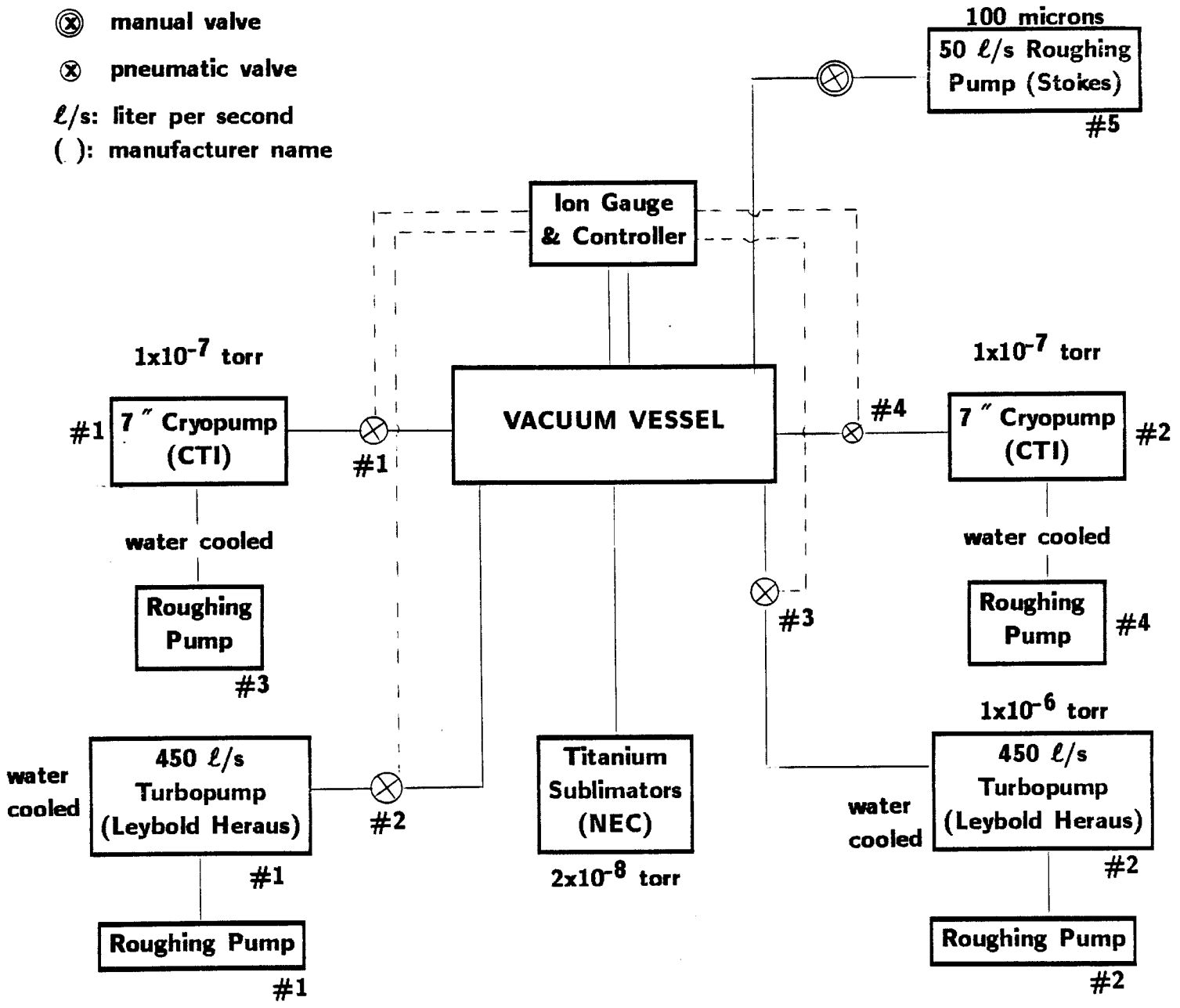

Fig. 2-7. Functional block diagram of Vacuum System.

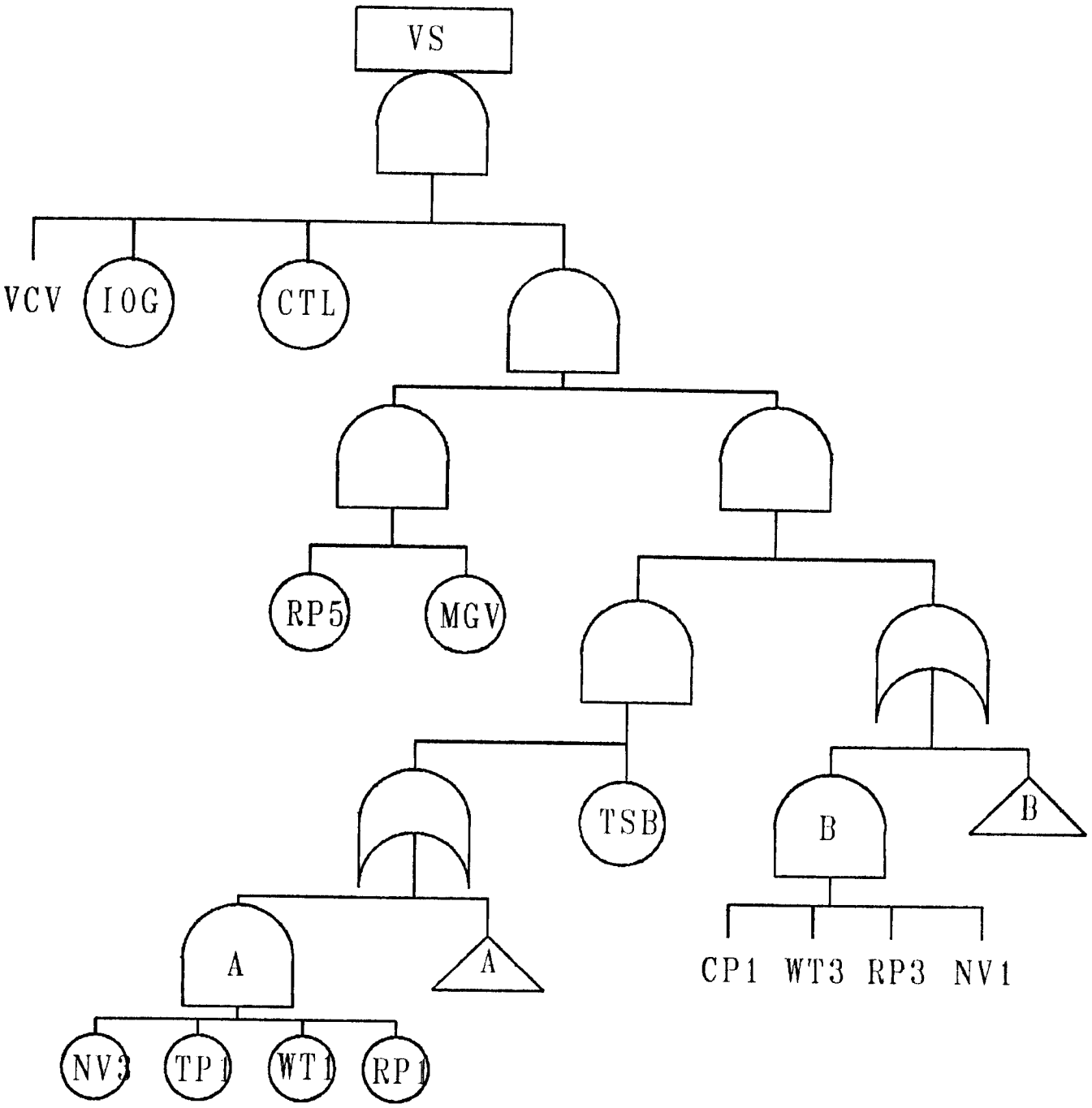

Fig. 2-8. Systems tree of Vacuum System.

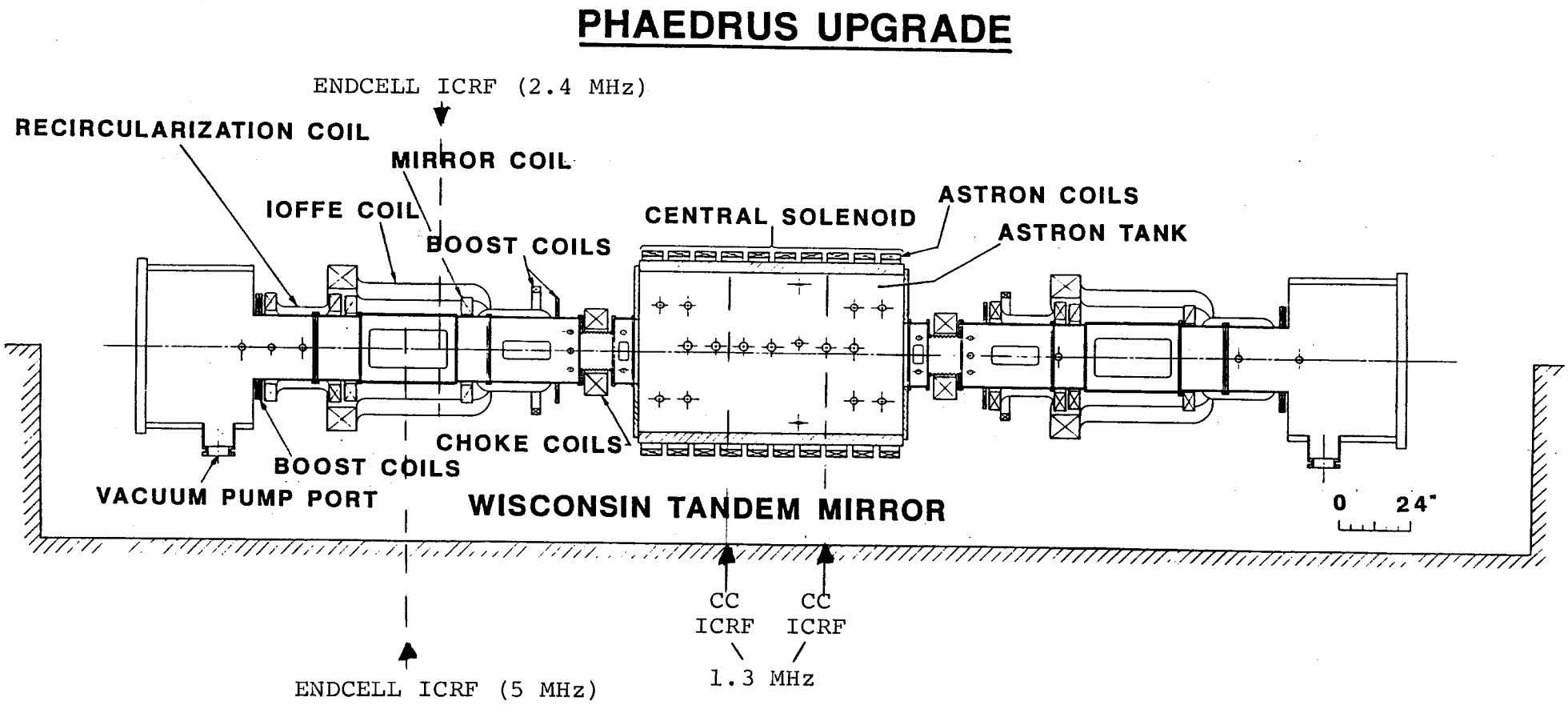

Fig. 2-9. Locations of ICRF antennas.

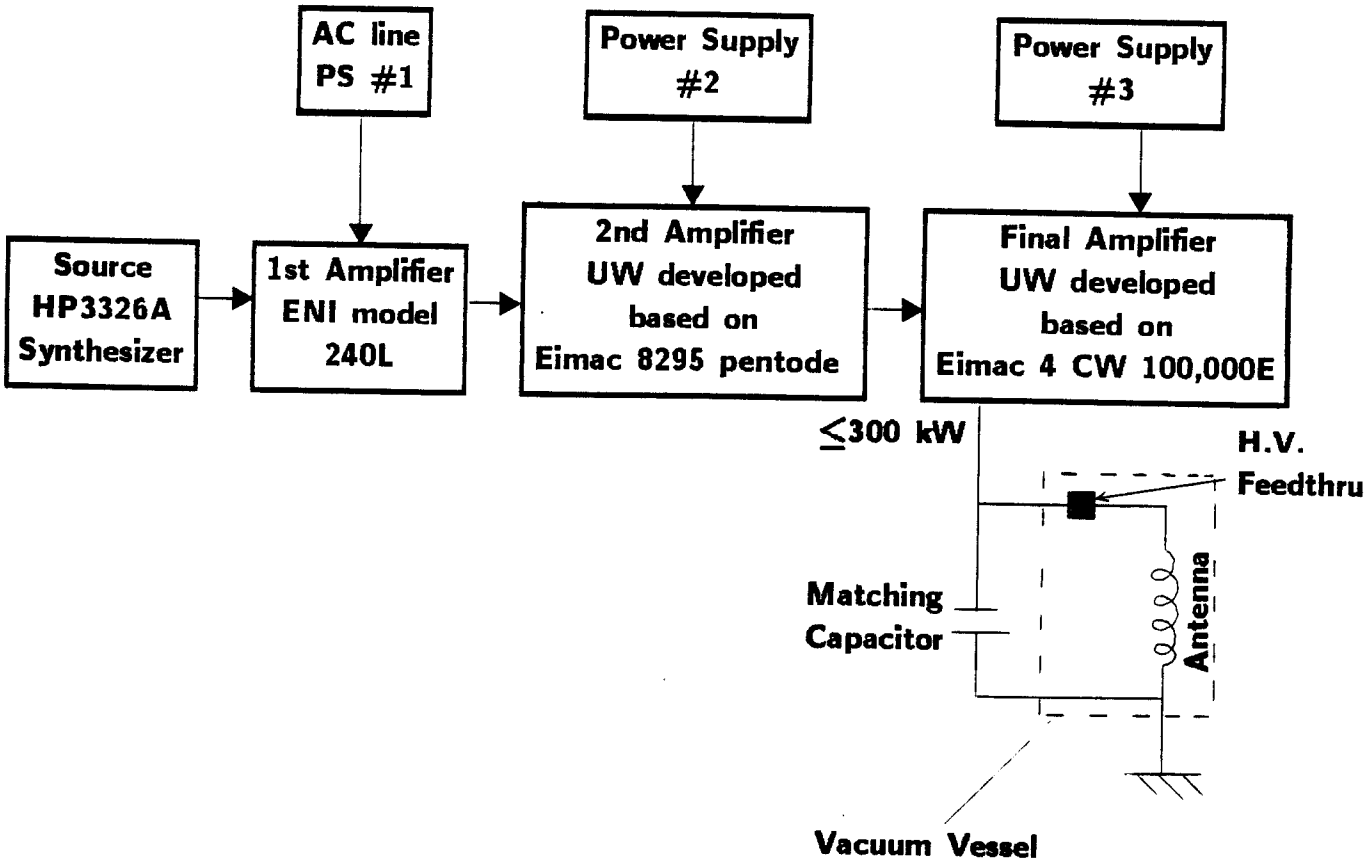

Fig. 2-10. (a) Functional block diagram of ICRF CC#1.

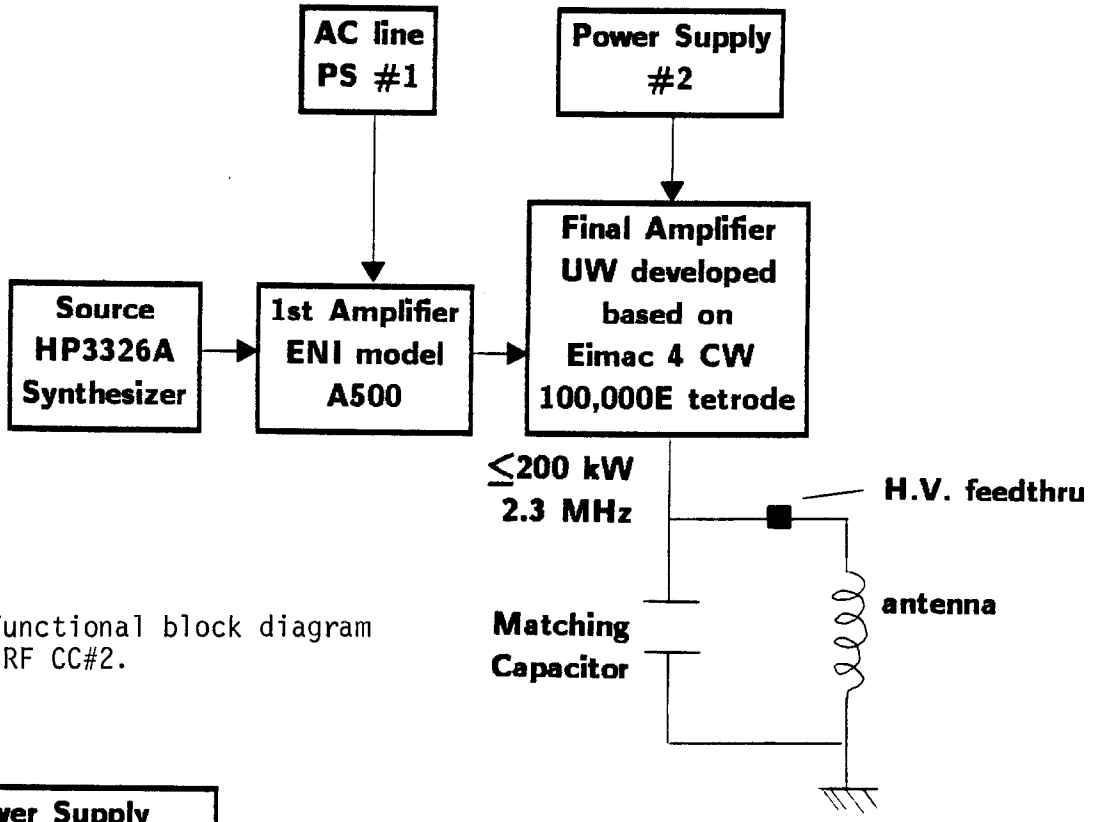

Fig. 2-10. (b) Functional block diagram of ICRF CC#2.

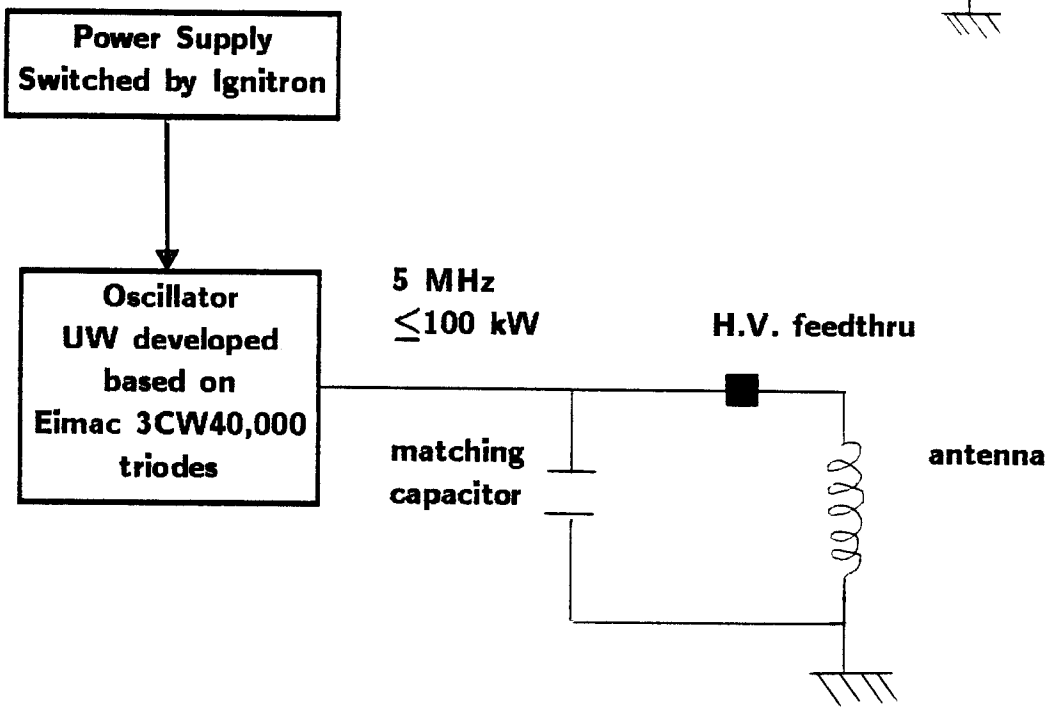

Fig. 2-10. (c) Functional block diagram of ICRF end cell.

vacuum vessel. A matching capacitor is located outside the vessel. The high voltage power (15 kV) is transmitted to the antennas through high voltage feedthrus. The second ICRF system (CC#2) has a similar structure to CC#1; but it has only two stages of amplifiers. The ICRF systems at the end cells have a different structure. An oscillator is used instead of a synthesizer and amplifiers. The power for the oscillator is supplied by three capacitor banks (30 microfarad at 20 kV). It is noted that many of the ICRF components were developed by the Phaedrus group. Final amplifiers and the oscillator are water-cooled. Table 2-4 gives a listing of ICRF components and Fig. 2-11 shows the systems tree.

2.2.5 Plasma Production System (PP)

Hydrogen gas puffed into the vacuum vessel by a gas puffing system is ionized by using several kW of 2.8 GHz ECRF. This produces low density and high temperature plasma. Then ICRF systems are turned on while keeping fueling by the gas puffing. Finally end cells are fueled by RF trapping of the central cell ion stream [22].

Only the ECH system (ECH), the gas puffing system (GPS), and gas supply (GAS) are included in the PP system. The ICRF is treated separately. The systems tree is given in Fig. 2-12.

2.2.6 Diagnostics System (DS)

The diagnostics system is the most complex subsystem in Phaedrus. There are ten subsystems as shown in Table 2-5. These are used to measure plasma parameters as summarized in Table 2-6.

Each of these systems is composed of many components. In particular the first four systems in Table 2-5 are very complex by themselves. Further

Table 2-4. Components in RF System

Components	ID
Central Cell ICRF #1	CC1
synthesizer	SYN
1st amplifier	1AP
2nd amplifier	2AP
final amplifier	FAP
antenna	ANT
matching capacitor	MCP
high voltage feedthru	HVF
power supply	PS#
cooling water	H2O
Central Cell ICRF #2	CC2
synthesizer	SYN
1st amplifier	1AP
final amplifier	FAP
antenna	ANT
matching capacitor	MCP
high voltage feedthru	HVF
power supply	PS#
cooling water	H2O
End Cell ICRF	EC#
oscillator	OST
power supply	PWS
antenna	ANT
matching capacitor	MCP
high voltage feedthru	HVF
cooling water	H2O

Table 2-5. Components in DS

Component	ID
Microwave interferometer	MII
Charge exchange energy analyzer	CEA
Time-of-flight energy analyzer	TOF
Thomson scattering system	TSS
Gridded end loss energy analyzer	GEL
Gridded energy analyzer	GEA
Diamagnetic loop	DIL
Langmuir probe/single	LPS
Langmuir probe/double	LPD
Self-emissive probe	SEP

Table 2-6. Diagnostics Used to Measure Plasma Parameters

Plasma Parameter	Measurement Device
density	MII
temperature	GEA, TSS, LPS, LPD
plasma beta	DIL
plasma radius	LPS
plasma potential	LPS, GEL, SEP
average ion energy	TOF, DIL, CEA
plasma axial scale length	DIL
end loss current density	GEL
end loss temperature	GEL

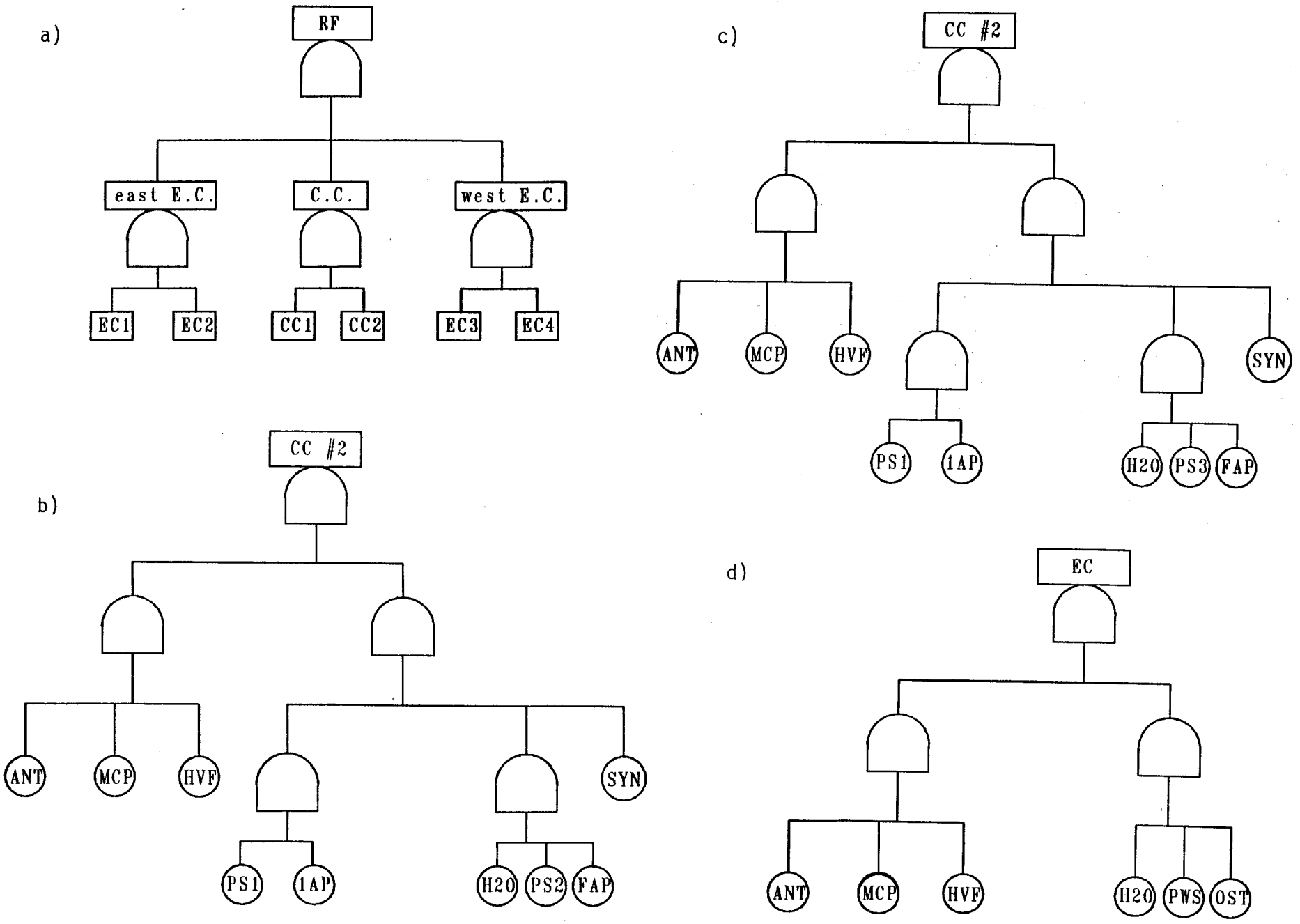

Fig. 2-11. Systems tree of ICRF System.

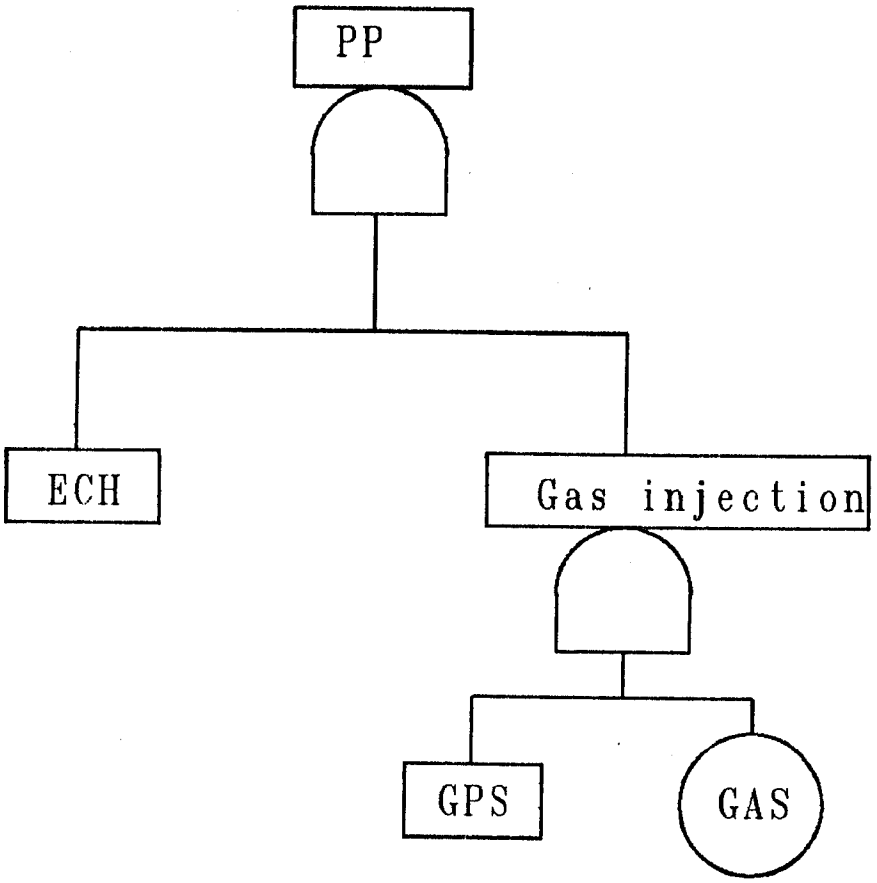

Fig. 2-12. Systems tree of Plasma Production System.

breakdown of these systems will be carried out in the next section. By regarding the above ten systems as components of the DS system, a systems tree given in Fig. 2-13 is created. The locations of diagnostics systems are illustrated in Fig. 2-14. Systems not shown in the figure are located at various places according to demand.

2.2.7 Data Acquisition and Computer System (DC)

The signals from diagnostics systems are processed at the CAMAC crates, transmitted from the crates to the CAMAC highway through optical fibers [25] and further processed at the MICROVAX-II computers. The data is analyzed and stored on magnetic tapes. The ETHERNET network is connected to the NMFECC network and a graphics display systems at the Phaedrus laboratory. The system is illustrated in Fig. 2-15. A listing of components is given in Table 2-7. Figure 2-16 shows a systems tree. It is noteworthy that the DC system is not used to control the entire Phaedrus experiment; its function is mainly data collection and processing. Feedback to the system is carried out manually by the operators.

2.2.8 Operators/Scientists (OP)

In addition to Prof. Hershkowitz there are a number of scientists and students who are responsible for subsystems. They are listed in Table 2-8. Some scientists and students are working with them. Figure 2-17 shows the systems tree.

2.3 Further Breakdown of Subsystems

2.3.1 Diagnostics System

Microwave interferometer, charge exchange energy analyzer, time-of-flight energy analyzer, and the Thomson scattering system are further broken down.

Table 2-7. Components in DC

Component	ID
CAMAC system	CAM
CAMAC crates/controller	CCC
CAMAC serial highway controller	CHC
MICROVAX II	MVA
VAX 11/750	VAX
ETHERNET system	ETH
Graphics display system	GRD
video monitor	VID
printer	PRT

Table 2-8. Scientists and Their Subsystems Responsibility

Name	ID	Subsystem ID
N. Hershkowitz	NH	Phaedrus
R.A. Breun	RAB	MC, DS-CEA
D.A. Brouchous	DAB	WS, DS-DIL
J.R. Ferron	JRF	DC, DS-MII
R. Majeski	RM	RF
J.A. Pew	JAP	VS, DS-TOF, DS-GEA
P.D. Brooker	PDB	DS-TSS
P.H. Probert	PHP	PP-ECH

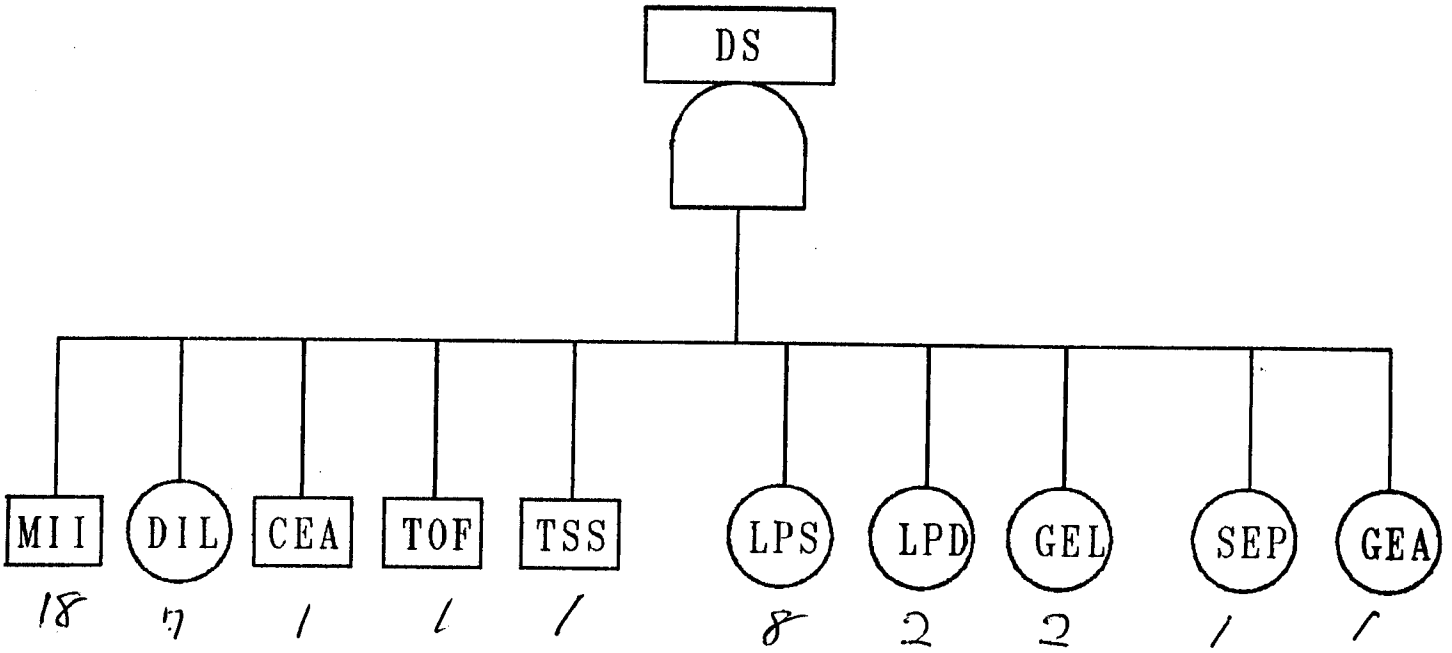

Fig. 2-13. Systems tree of Diagnostic System.

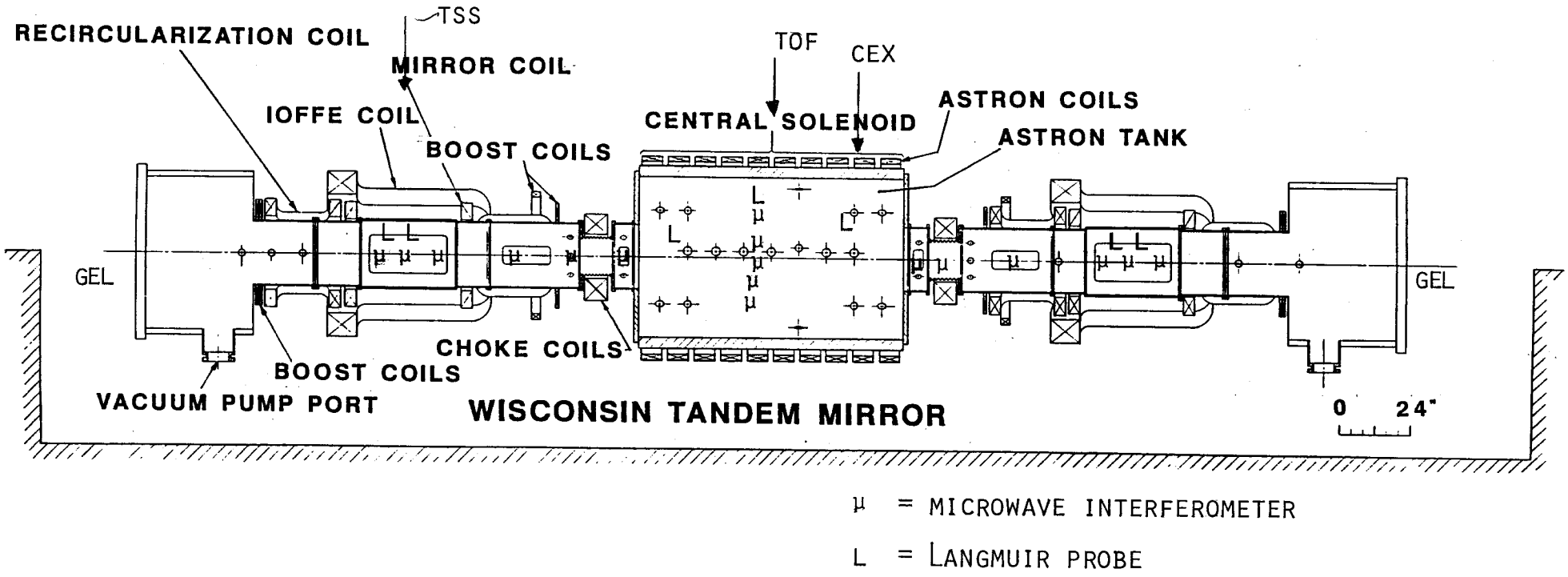

Fig. 2-14. Locations of Diagnostics System.

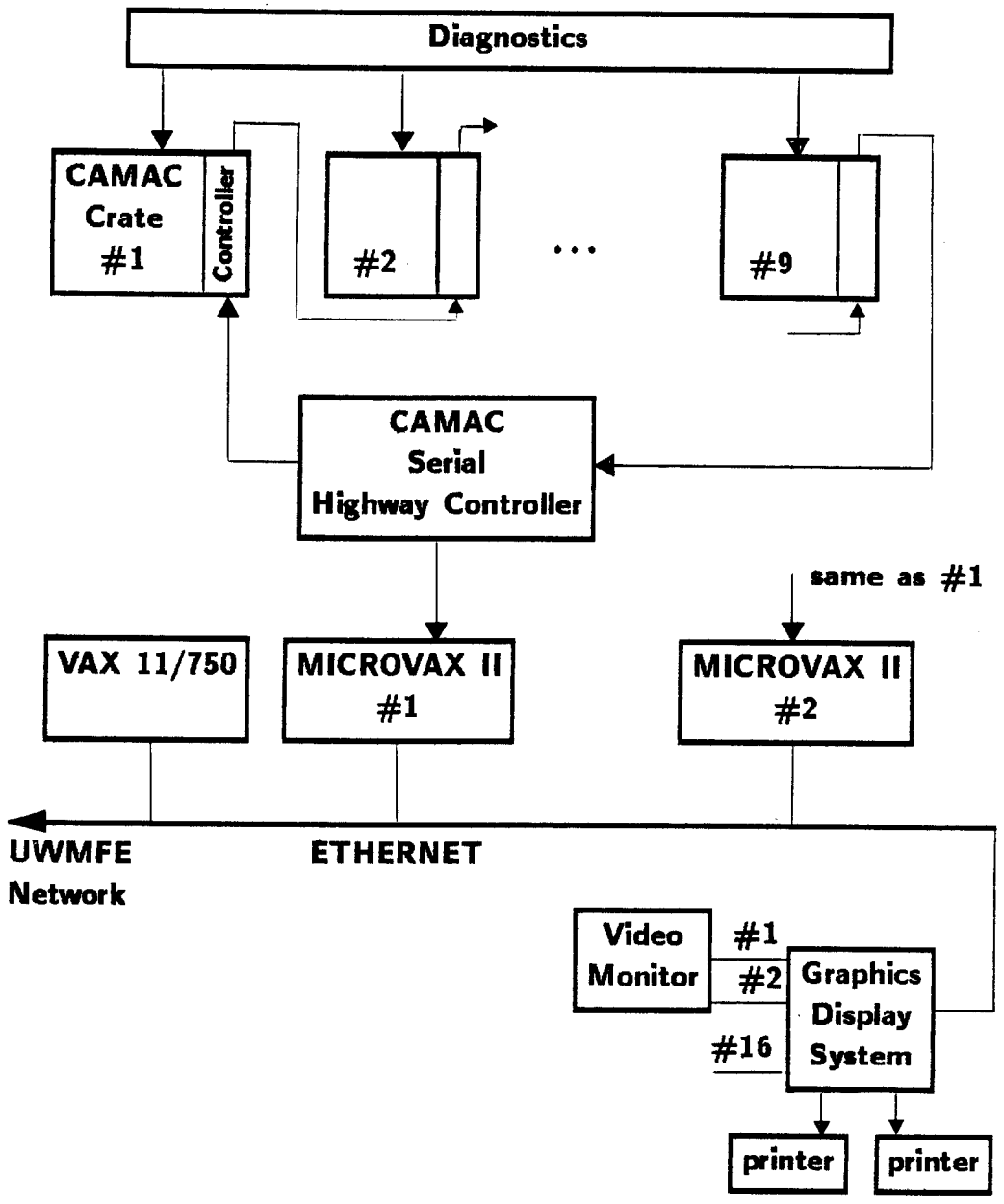

Fig. 2-15. Functional diagram of Data Acquisition and Computer System.

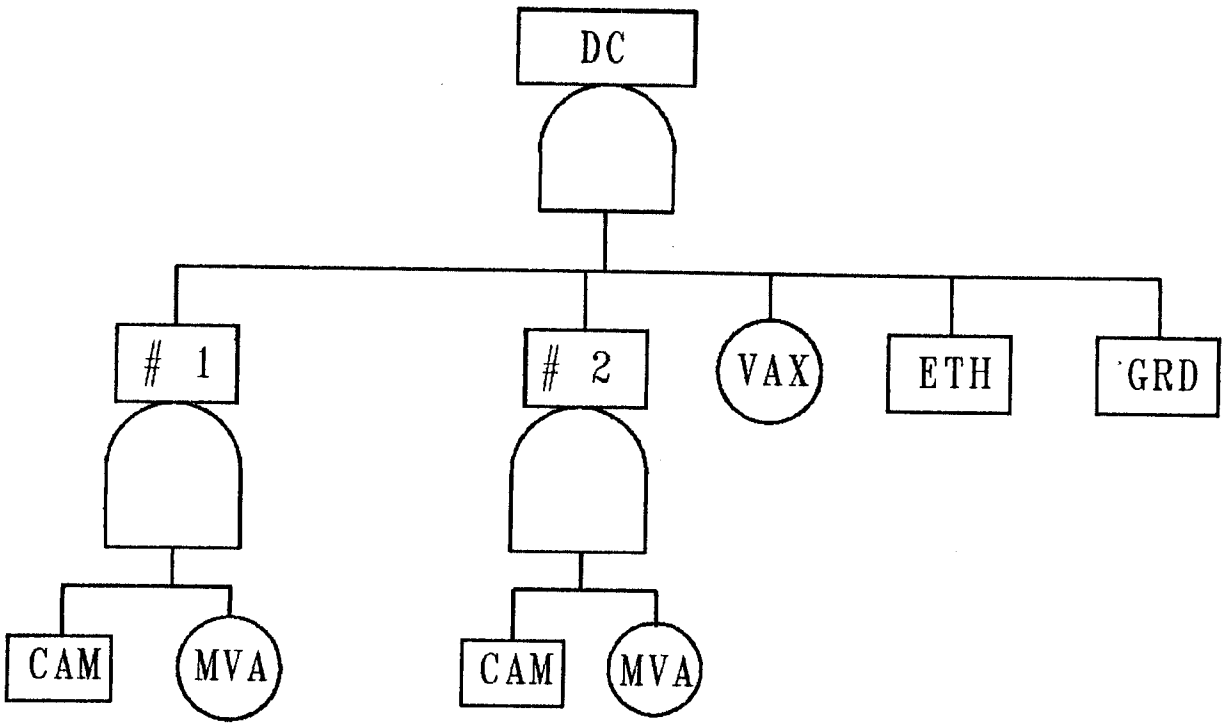

Fig. 2-16. Systems tree of Data Acquisition and Computer System.

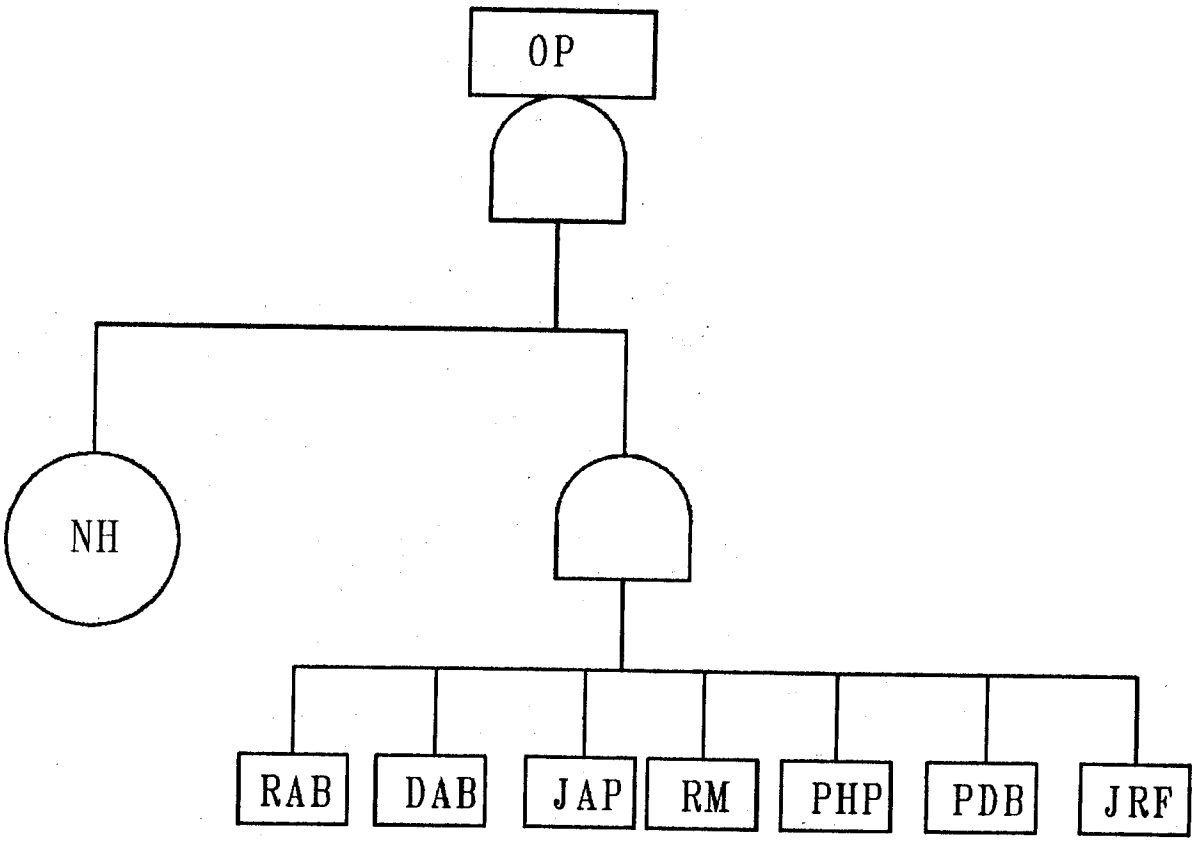

Fig. 2-17. Systems tree of Operators/Scientists.

Functional block diagrams and listings of components of these systems are given in Figs. 2-18 to 2-21 and Tables 2-9 to 2-12.

2.4 Operation Model

2.4.1 Long Term Model

Phaedrus was constructed in the late 1970's and experiments began around 1980. In 1985 a major modification in coil configuration was completed. The facility was closed for five months for that modification. Except for this period the device has been operated continuously.

Several experiments are set up and performed simultaneously by groups of people. The machine time is allocated to different experiments if they cannot be carried out at the same time. The number of experiments varies in time. Some last a long time and some are completed in a short period.

Experiments are performed at any time by the researcher's decision. Typically the entire system is operated from 8:30 am to 5 pm five days a week.

Maintenance is carried out whenever failures are noticed. Scheduled maintenance is not particularly planned.

In summary the operation of Phaedrus is very random and it is doubtful if any general model can be created except the operation mode discussed in the following section.

2.4.2 Pulse Model

Phaedrus is a pulsed machine. This means that plasma is produced for millisecond periods and all subsystems are adjusted to this time scale. The pulse length does not vary for different experiments. The time sequence of

Table 2-9. Components in MII

Component	ID
transmission horn	TRH
receiving horn	RCH
waveguide	WGD
gunn oscillator	OSC
balanced mixer	MIX
phase shifter	PSH
attenuator	ATT
amplifier	AMP
phase comparator	CPM
sawtooth waveform generator	GEN
power supply	PS#

Table 2-10. Components in CEA

Component	ID
gate valve	GVL
vacuum vessel	VVL
vacuum pump	VPP
gas puffing system	GPS
stripping cell	STC
electrodes	ELC
ion collector	ICL
plastic scintillator	PSC
photo multiplier tube	PMT
power supply	PS#

Table 2-11. Components in TOF

Component	ID
vacuum vessel	VVL
gate valve	GV#
chopper	CHP
motor	MTR
ion gauge	IOG
electron multiplier	ELM
turbo pump	TPP

Table 2-12. Components in TSS

Component	ID
laser source	LAS
lense	LEN
vacuum photodiode	VPH
pulser	PLS
glasses	GLS
blue glass dumper	BGD
polychrometer	PLC
photomultiplier	PHM
power supply	PS#
current integrating AD convertor	ADC

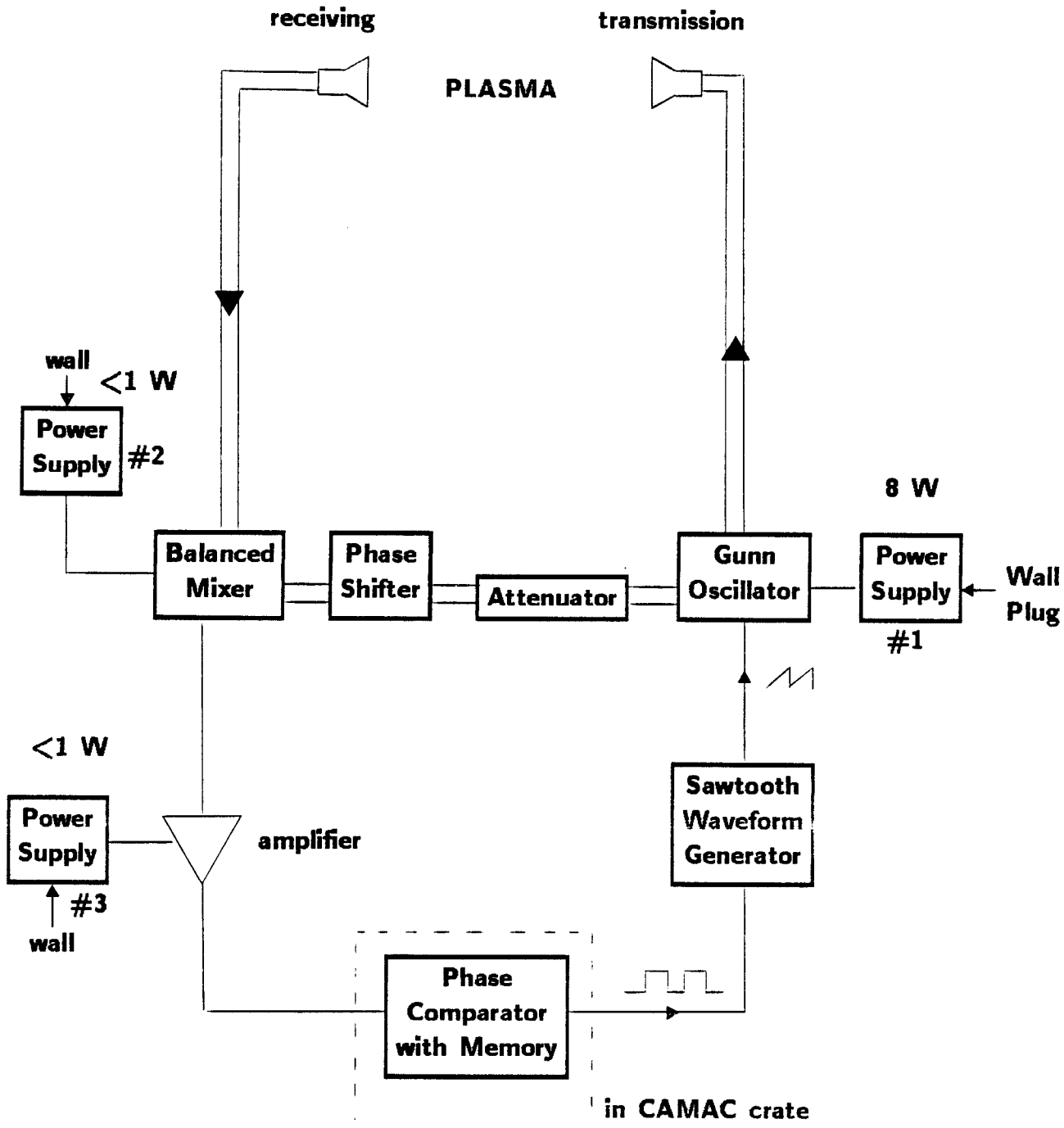

Fig. 2-18. Functional block diagram of microwave interferometer.

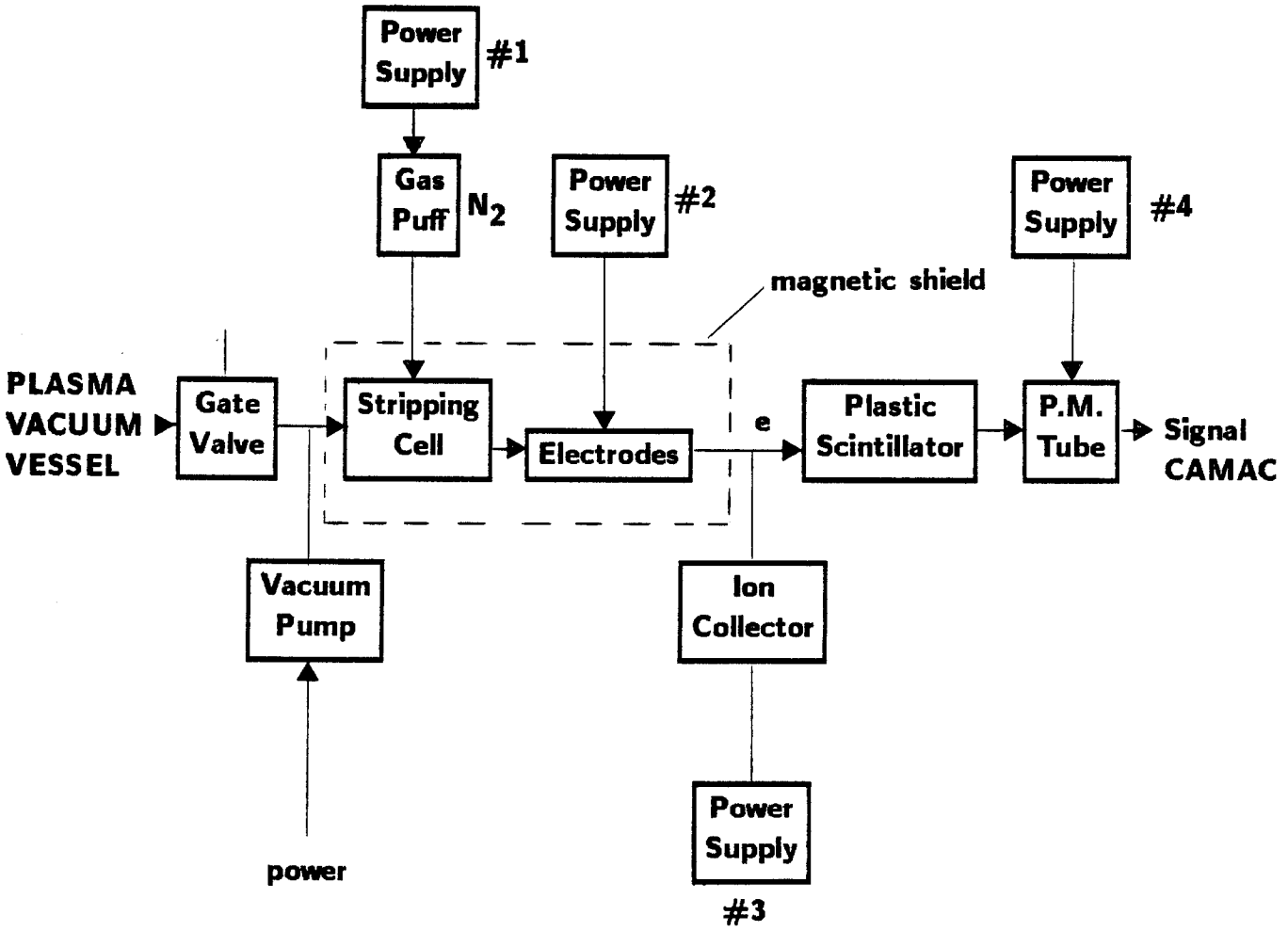

Fig. 2-19. Functional block diagram of charge exchange analyzer.

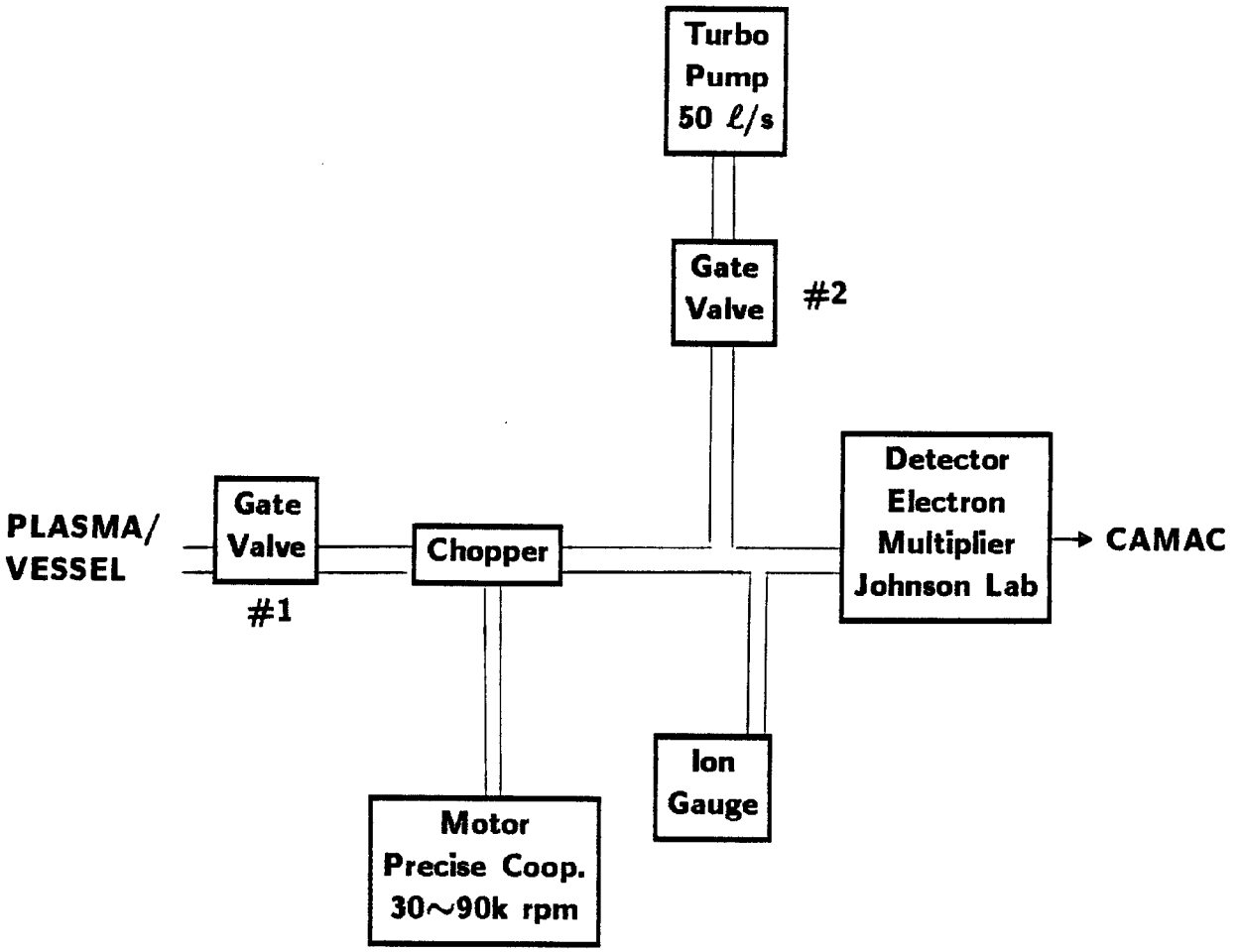

Fig. 2-20. Functional block diagram of time-of-flight energy analyzer.

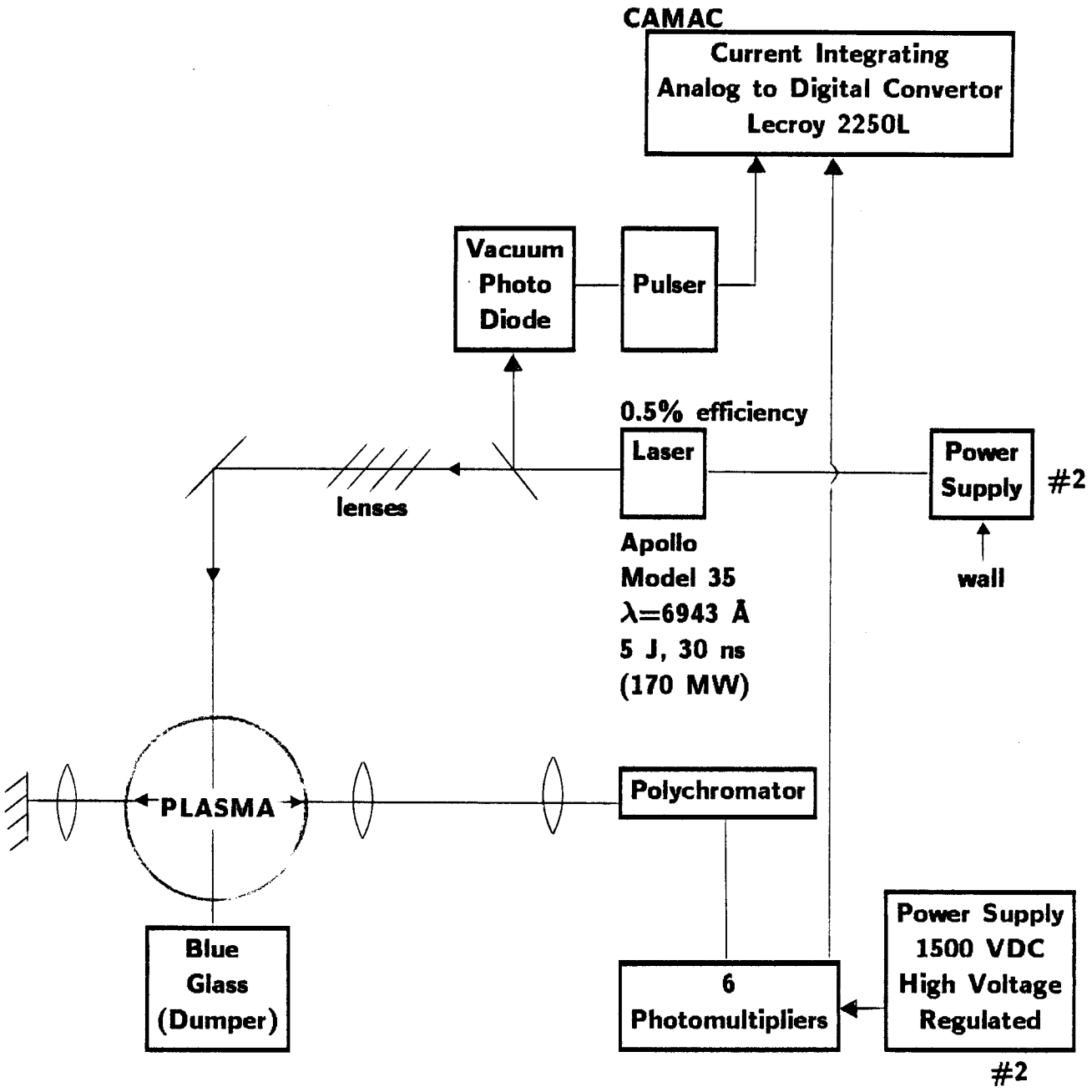

Fig. 2-21. Functional block diagram of Thomson scattering system.

Table 2-13. Mode of Operation

Component ID	Operation mode
MC	pulse of 5 seconds
WS	continuous
VS	continuous
RF	pulse of 20 ms
PP	pulse of 5 ms
DS	pulse of 20 ms
DC	pulse of 20 ms
OP	continuous

the subsystem operations may be different for different experiments. Figure 2-22 shows the timing of subsystem operation for a particular experiment. Although the experiments are discrete in time, some subsystems are continuously operated. Operation modes of the subsystems are summarized in Table 2-13.

2.5 Failure/Repair Model

2.5.1 Failure Model

With a few exceptions most of the components are operated in pulse mode. There is a rather long period between successive pulses. Thus a special caution must be paid in using conventional concepts of failure rates/probabilities. In this study the failure rate r(t), which is the probability that a system fails at time t, is used for systems operated continuously. Meanwhile, for systems in pulse operation we use the failure probability p_i, which is defined as the probability that a system fails at the i-th shot.

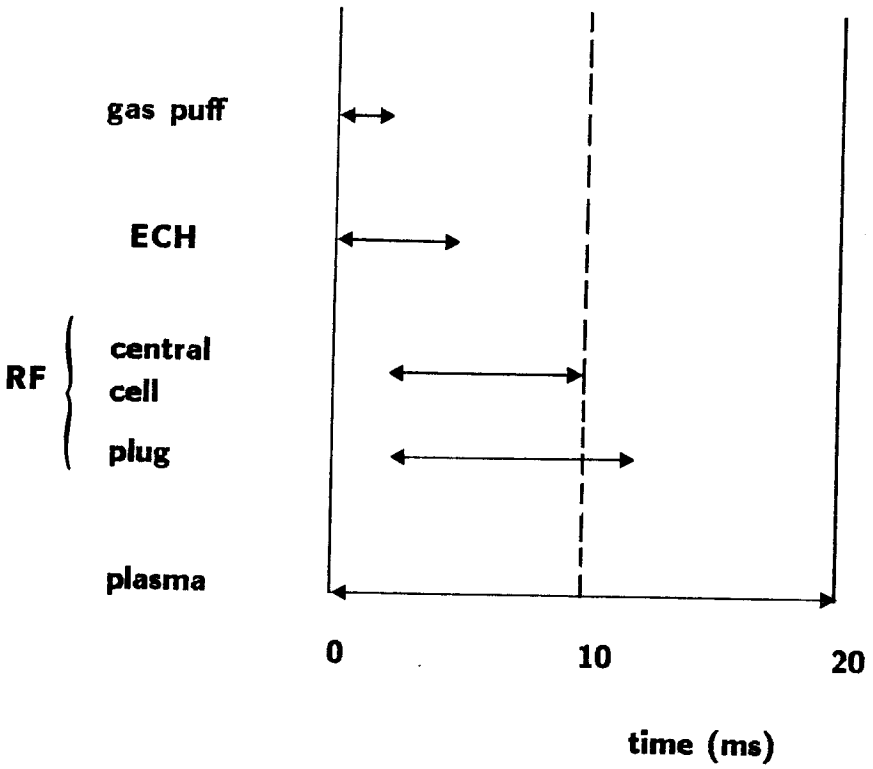

Fig. 2-22. Time sequence for RF stabilization experiment.

2.5.2 Repair Model

We assume that a repair activity is immediately started when a system fails. Since the repair process is always continuous in time, we can use the standard concept of repair rate.

3. RELIABILITY DATA

3.1 Data Collection

Reliability data needed to analyze Phaedrus does not exist. We are planning to collect data in the future. For the initial analysis we shall use the data based on researchers' experience at Phaedrus. The staff has experience with the system ranging from a few months to several years. Thus it is possible to obtain failure/repair data from them. Their knowledge can be considered as data statistically processed in their own minds. We distributed the data solicitation forms shown in Fig. 3-1. The results are summarized in Table 3-1.

Some comments should be made on the data:

(i) Only major failure modes, which were noticed by the Phaedrus scientists, are given in the table.

(ii) There is no correspondence between the failure modes and MTTF/MTTR when there are more than two failure modes.

(iii) MTTF and MTTR are not statistical averages. Some MTTF may be the time to failure of a system that had failed only once so far.

(iv) Some components have never failed. In the table this is indicated by "none" followed by the time length operated in parentheses.

(v) It is not clear whether MTTF is actually MTTF or MTBF. Nevertheless, the difference does not introduce much uncertainty because the MTTR is much shorter than the MTTF.

(vi) The failure frequency very much depends on how a system was operated; but sufficient data regarding the operational history is not available.

Table 3-1

Component ID	Failure Mode	MTTF	MTTR
MC-FS#	none (8 years)		
MC-TR1	none (8 years)		
MC-TR2			
MC-TR3	none (8 years)		
MC-TR4	none (2 years)		
MC-CR1	none (8 years)		
MC-CB2	none (2 years)		
MC-CB3	fail to close	4 years	1 month
MC-ERB			
MC-MGE			
MC-PS#			
MC-PH#	fuse failure	1 year	1 day
MC-TM#	relay failure	6 years	1 day
MC-SC#		2-4 failures out of 42 units per year	1-2 hours
MC-CCC	none (8 years)		
MC-SCA	short circuit	1 for 8 years	1 week - 2 years
MC-MSC	water leak	1 for 8 years	1 week - 2 years
MC-CHC	none (1.5 years)		
MC-SCB	short circuit	1 for 8 years	1 week - 2 years
MC-COL	none		
MC-IOF	short circuit	1 for 8 years out of 2 units	1 week - 2 years
WS-CWS			
WS-DIS			
WS-PMP			
WS-PIP			
WS-VLV			
VS-VCV	leaks	2 weeks	1.5 hr/wk
VS-RP5	none (6 years)		
VS-RP#	none		
VS-CP#	wear out	5 years	1 week
VS-TP#	none		
VS-MGV	none		
VS-NV#	not close	4 years	3 hours
VS-TSB	Ti depleted	1 month	200 minutes
VS-IOG	filament burn-out	2 years	10 minutes
VS-CTL	none		
VS-WAT			
RF-CC1-SYN	none (9 months)		
RF-CC1-1AP	none (1 year)		
RF-CC1-2AP	arcing	10 weeks	1-2 hours

Table 3-1. (continued)

Component ID	Failure Mode	MTTF	MTTR
RF-CC1-FAP	arcing	1 week	1-2 hours
RF-CC1-ANT	none		
RF-CC1-MCP	none (9 months)		
RF-CC1-HVF	none (6 months)		
RF-CC1-PS#	none		
RF-CC1-H2O			
RF-CC2-SYN	none		
RF-CC2-1AP	none		
RF-CC2-FAP	arcing	1 week	1- 2 hours
RF-CC2-ANT	none		
RF-CC2-MCP	none		
RF-CC2-HVF	none		
RF-CC2-PS#	none		
RF-CC2-H2O			
RF-EC#-OST	arcing	2-4 weeks	1-4 hours
RF-EC#-PWS	ignition failure	1 month	1 hr - 1 day
RF-EC#-ANT	none		
RF-EC#-MCP	none		
RF-EC#-HVF	none		
RF-EC#-H2O			
PP-ECH			
PP-GPS			
PP-GAS			
DS-MII	out of tune	4 weeks	1/2 hour
	receiving horn failure	2 months	2 hours
DS-CEA	vacuum pump failure	5 months	1-2 days
DS-TOF	none		
DS-TSS			
DS-GEL			
DS-GEA			
DS-DIL			
DS-LPS			
DS-LPD			
DS-SEP			
DC-CAM-CCC	electronic failure	1 year	1 month
DC-CAM-CHC	electronic failure	1 year	1 month
DC-MVA	none		
DC-VAX	none		
DC-ETH	none		
DC-GRD	bad contacts	6 months	1/2 hour

Data Collection Form						
subsystem:				DATE: / /		
Component name	Failure mode what happened?	Failure cause	time to failure	CL	time to repair or replacement	CL
CL = A : >95%, B :80-95, C :60-80, D:40-60, E:<40. Confidence level						

Fig. 3-1. Sample form for data solicitation.

3.2 CREDO Data Management System

The adapted CREDO system which uses the data collection formats similar to the original CREDO system developed for the fast breeder reactor program was designed for the Tritium Systems Test Assembly (TSTA) [19]. The adapted version of CREDO is portable; in fact, it runs on an IBM-PC computer with the Knowledgeman data management program and needs about 800 kbytes of memory for storing the program. The system has also been adapted to the Phaedrus experiment. For this purpose some modifications are made. Event reporting forms for the original CREDO system are used instead of forms prepared for the TSTA facility specifically. The auxiliary part in the engineering data base is eliminated. How to use the CREDO system at the Phaedrus site has not been decided. As a reference, however, a procedure is proposed. It is illustrated in Fig. 3-2. To gather data constantly, personnel specifically for that purpose must be hired or an automated data collection technique must be developed.

3.3 Operation Records

One of goals of the present analysis is to predict the availability of Phaedrus. The predicted availability must be evaluated by comparing with actual performance so that the models, analysis method, and data used could be validated. For this purpose the operation log books were looked into. There are two kinds of log books. One of them (Log A) contains signals from diagnostics systems, RF current and voltage signals, ECRH power signal, and others. Which signals are recorded in the log depends on the type of experiments. An example is given in Fig. 3-3. Another log book (Log B) shows which parameters of subsystems (RF voltage, magnetic coil current, etc.) are changed for each shot. A copy of the Log B is given in Fig. 3-4.

Reliability Data Collection Scheme for PHAEDRUS

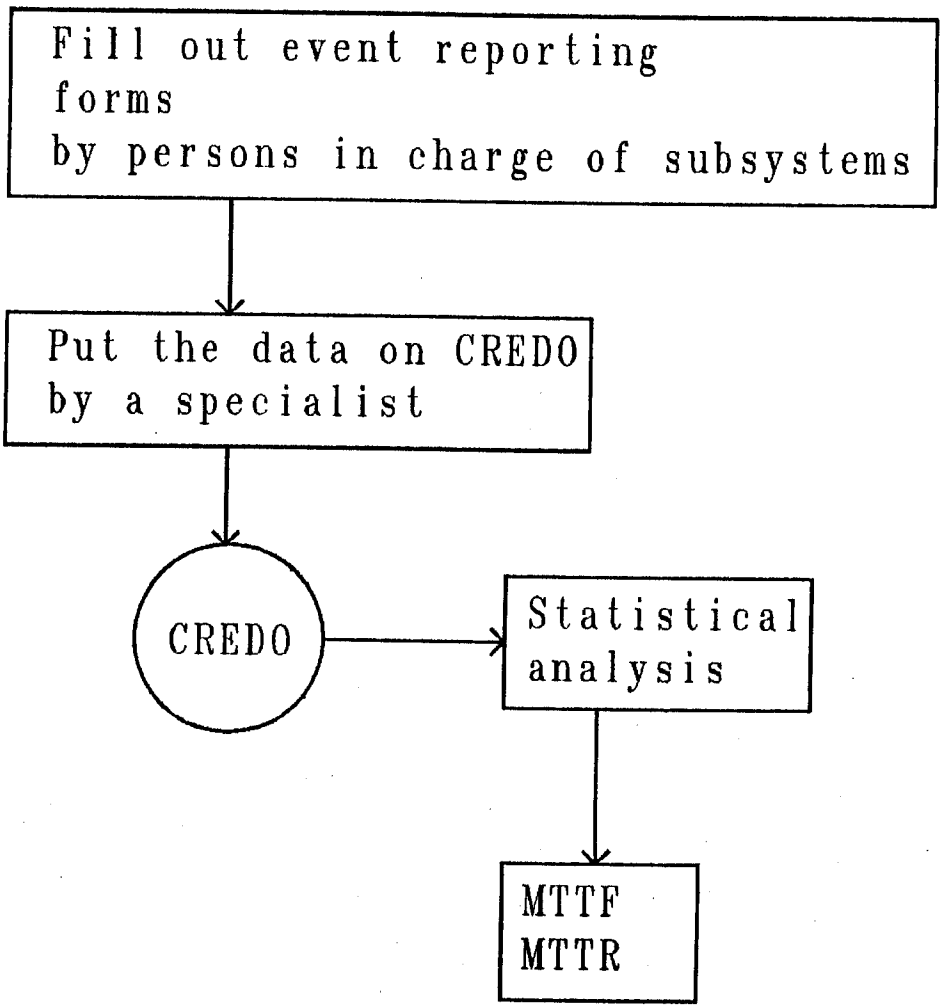

Fig. 3-2. Proposed data collection scheme for Phaedrus.

56778

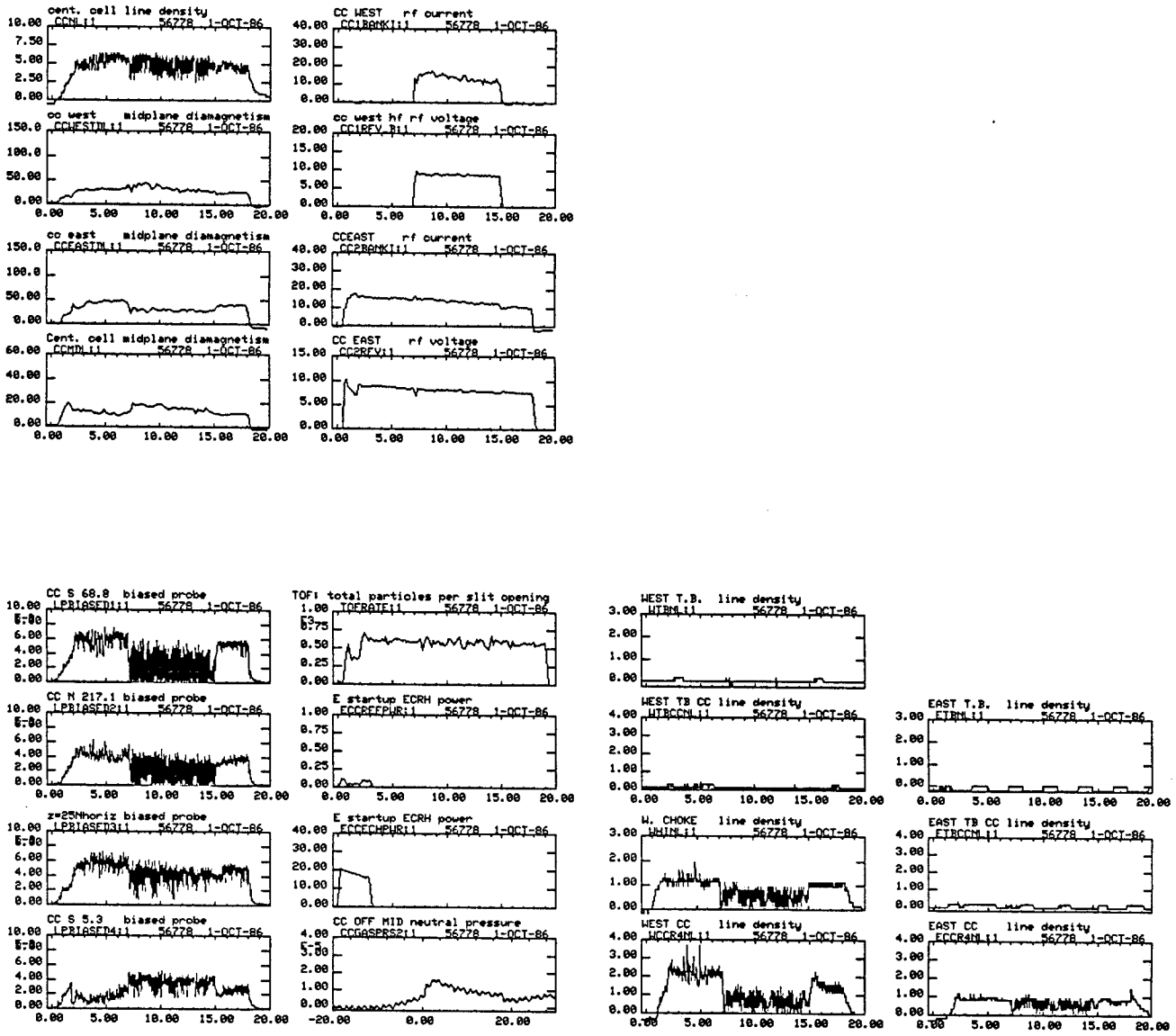

Fig. 3-3. Typical data in the operation log book A.

10/1/86
JJ 1 5

Items Varied

2.123217H/.327TH2

Shot #	$V_{cc\phi_1}$	$V_{cc\phi_2}$	gas		LP1	LP2	LP3	LP4	Comments
56661	off	1.4V=V_D 10KV	1psi t=80 Δt=30ms 800K		r=14	r=14	r=14	r=9	cc=410K=1078A choke=630K (G)(E)
62									
63									choke=600K
64									
65									choke=570K
66									
67									choke=540K=1385A
68									
69									choke=510K=1308A
70									
71									choke 480K=1231A
72									(G) cc=430K=1098A (GE)
73									
74									cc=450K=1150A
75									
76									c=470K=1200A
77									
78									cc=500K=1225A
79									
80									cc=430K choke=480K (I
no plasma 81			r=8.2 Δt=30ms						ECH fault
82									
83		13.5KV							
84									
85		V_D=1.4V							
86									yest 2 temp MAXIMUM
87		14.5KV							
88									

Fig. 3-4. Typical data in the operation log book B.

Let us look at only signals of the central cell line-density and the time-of-flight (TOF). We consider that the plasma (density) is normal if the density signal is flat at the magnitude of 5.0 for the entire pulse, it is degraded if the signal is around 2.5, and it is failed if the signal is almost 0 or the pulse is much shorter than 20 ms. A similar evaluation standard is set for the TOF signal; the plasma is normal if the signal is about 0.5, it is degraded if about 0.25, and otherwise it is failed.

The operation log (Log A) for 28 September 1986 to 1 October 1986 (total 281 shots) was examined. The data is summarized according to the definitions of states described above. Table 3-2 shows the result. The ratios of the number of each state to total number of shots are calculated for 29 September and 1 October. The first two days of the experiment were spent in preparation by adjusting subsystems. It is better to exclude the performance on these two days. The table indicates that about 50% of the shots were successful, about 20% were failed, and the others were degraded.

There are two uncertainties in this analysis. First, the states of the density and TOF signals do not always tell the cause clearly; the cause may be intentional, i.e. parameters of subsystems are changed to obtain the degraded state, rather than being due to the failure of subsystems. To clarify this point, the Log B was also examined. The records indicate that for the shot number 56534 to 56801 there were only four unsuccessful shots: three due to the failure of the ECH system and one due to the failure of the RF system. Thus, the success ratio is 264/268 (= 98.5%). Second, the classification of signals to three states is not free of ambiguity; for example, which state is it if the signal level is high enough for the normal state but very noisy?

Table 3-2. Summary of Operation (09/28/86-10/01/86)

Shot #	c.c. line-density			TOF		
	normal	degraded	failed	normal	degraded	failed
(28-SEP-86)						
56521-56522	0	0	2			
(29-SEP-86)						
56523-56532	2	2	5			
533- 542	6	4	0			
543- 551	7	2	0			
(30-SEP-86)						
56552-56561	4	1	5			
562- 571	1	4	5			
572- 581	10	0	0			
582- 591	0	10	0			
592- 601	10	0	0			
602- 611	10	0	0			
612- 621	0	8	2			
622- 631	0	8	2			
632- 641	4	3	3	4	4	2
642- 651	8	1	1	2	7	1
652- 661	7	3	0	7	3	0
110 shots	54	38	18			
ratio	0.49	0.35	0.16			
(01-OCT-86)						
56662-56671	9	0	1	9	0	1
672- 681	9	0	1	7	2	1
682- 691	10	0	0	10	0	0
692- 701	3	0	7	3	7	0
702- 711	5	2	3	0	10	0
712- 721	0	5	5	0	6	4
722- 731	7	3	0	7	3	0
732- 741	9	0	1	9	1	0
742- 751	5	5	0	5	5	0
752- 761	6	4	0	10	0	0
762- 771	7	3	0	2	6	2
772- 781	3	5	2	3	4	3
782- 791	0	8	2	0	8	2
792- 801	4	3	3	0	9	1
140 shots	77	38	25	65	61	14
ratio	0.55	0.27	0.18	0.46	0.44	0.1

4. RELIABILITY ANALYSIS

4.1 Symbolic Analysis

Based on the systems tree developed in Section 2 a systems tree for Phaedrus is created as shown in Fig. 4-1. Only component ID numbers are given in the figure. Correspondence of the ID number and components are given in Table 4-1. The table also gives the number of units, the number of redundant units if any, the failure rate λ, and the repair rate μ. Here we assume constant failure rates and repair rates.

Calculations are performed by using the symbolic availability analysis program REDFOR with the symbolic manipulation program REDUCE [17]. Results are shown in Table 4-2. Steady-state availabilities, BIRNBAUM and Criticality importances of components, subsystems, and the Phaedrus system are given. Importances are measures that indicate how much change in the availability of the entire system occurs when the availability of a component is increased or decreased. A large importance implies that a small increase in the availability of the component may significantly increase the availability of the entire system. The steady-state availability means the availability when times between successive pulses, scheduled maintenance and down time due to other reasons are ignored. The values do not indicate the real performance of systems. We can find, however, which systems are weak from the reliability point of view and which systems are important to increase the system reliability when values of components are compared one another.

By observing Tables 4-2 and 4-3 the following conclusions can be drawn:

(i) Assume that the steady-state availability is equivalent to the success rate of the shots; that is, 57% availability means that there are 57 successful shots out of 100 shots.

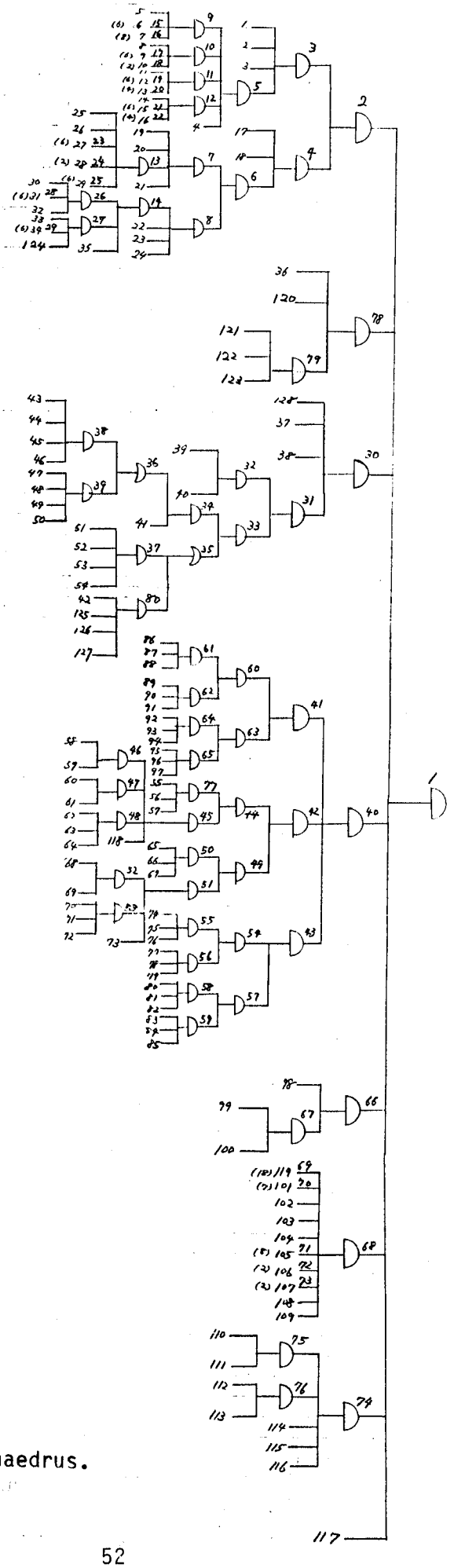

Fig. 4-1. Systems tree of Phaedrus.

Table 4-1. Component Data Used in Analysis

Component ID	ID number in tree	Number of units	Redundancy	λ (1/hr)	μ (1/hr)
MC-FS1	22	1	0	1.0E-7	1.0E-1
MC-FS2	21	1	0	1.0E-7	1.0E-1
MC-TR1	3	1	0	1.0E-7	1.0E-1
MC-TR2	18	1	0	1.0E-7	1.0E-1
MC-TR3	23	1	0	1.0E-7	1.0E-1
MC-TR4	20	1	0	1.0E-7	1.0E-1
MC-CB1	2	1	0	1.0E-7	1.0E-1
MC-CB2	19	1	0	1.0E-7	1.0E-1
MC-CB3	24	1	0	2.9E-5	1.4E-3
MC-ERB	1	1	0	1.0E-7	1.0E-1
MC-MGE	17	1	0	1.0E-7	1.0E-1
MC-PS1	5	1	0	1.0E-7	1.0E-1
MC-PS2	8	1	0	1.0E-7	1.0E-1
MC-PS3	11	1	0	1.0E-7	1.0E-1
MC-PS4	14	1	0	1.0E-7	1.0E-1
MC-PH1	26	1	0	1.1E-4	4.0E-2
MC-PH2	30	1	0	1.1E-4	4.0E-2
MC-PH3	33	1	0	1.1E-4	4.0E-2
MC-TM1	4	1	0	1.9E-5	4.0E-2
MC-TM2	25	1	0	1.9E-5	4.0E-2
MC-TM3	35	1	0	1.9E-5	4.0E-2
MC-SC1	6	6	0	1.1E-5	5.0E-1
MC-SC2	9	6	0	1.1E-5	5.0E-1
MC-SC3	12	6	0	1.1E-5	5.0E-1
MC-SC4	15	6	0	1.1E-5	5.0E-1
MC-SC5	29	6	0	1.1E-5	5.0E-1
MC-SC6	31	6	0	1.1E-5	5.0E-1
MC-SC7	34	6	0	1.1E-5	5.0E-1
MC-CCC	7	8	0	1.0E-7	1.0E-1
MC-SCA	10	2	0	4.1E-6	1.4E-3
MC-MSC	13	4	0	4.1E-6	1.4E-3
MC-CHC	16	2	0	1.0E-7	1.0E-1
MC-SCB	27	6	0	4.1E-6	1.4E-3
MC-COL	28	2	0	1.0E-7	1.0E-1
MC-IF1	32	1	0	8.2E-6	1.4E-3
MC-IF2	124	1	0	8.2E-6	1.4E-3
WS-CWS	36	1	0	1.0E-7	1.0E-1
WS-DIS	120	1	0	1.0E-7	1.0E-1
WS-PMP	121	1	0	1.0E-7	1.0E-1
WS-PIP	122	1	0	1.0E-7	1.0E-1
WS-VLV	123	1	0	1.0E-7	1.0E-1

Table 4-1. (continued)

Component ID	ID number in tree	Number in units	Redundancy	λ (1/hr)	μ (1/hr)
VS-VCV	128	1	0	3.0E-3	3.3E-1
VS-RP5	39	1	0	1.0E-7	1.0E-1
VS-RP1	46	1	0	1.0E-7	1.0E-1
VS-RP2	50	1	0	1.0E-7	1.0E-1
VS-RP3	53	1	0	1.0E-7	1.0E-1
VS-RP4	126	1	0	1.0E-7	1.0E-1
VS-CP1	51	1	0	2.3E-5	6.0E-3
VS-CP2	42	1	0	2.3E-5	6.0E-3
VS-TP1	44	1	0	1.0E-7	1.0E-1
VS-TP2	48	1	0	1.0E-7	1.0E-1
VS-MGV	40	1	0	1.0E-7	1.0E-1
VS-NV1	54	1	0	2.8E-5	3.3E-1
VS-NV2	127	1	0	2.8E-5	3.3E-1
VS-NV3	43	1	0	2.8E-5	3.3E-1
VS-NV4	47	1	0	2.8E-5	3.3E-1
VS-TSB	41	1	0	1.4E-3	3.3E-1
VS-IOG	37	1	0	5.7E-5	6.0E-0
VS-CTL	38	1	0	1.0E-7	1.0E-1
VS-WT1	45	1	0	1.0E-7	1.0E-1
VS-WT2	49	1	0	1.0E-7	1.0E-1
VS-WT3	52	1	0	1.0E-7	1.0E-1
VS-WT4	125	1	0	1.0E-7	1.0E-1
RF-CC1-SYN	118	1	0	1.0E-7	1.0E-1
RF-CC1-1AP	59	1	0	1.0E-7	1.0E-1
RF-CC1-2AP	61	1	0	6.0E-4	5.0E-1
RF-CC1-FAP	64	1	0	6.0E-3	5.0E-1
RF-CC1-ANT	55	1	0	1.0E-7	1.0E-1
RF-CC1-MCP	56	1	0	1.0E-7	1.0E-1
RF-CC1-HVF	57	1	0	1.0E-7	1.0E-1
RF-CC1-PS1	58	1	0	1.0E-7	1.0E-1
RF-CC1-PS2	60	1	0	1.0E-7	1.0E-1
RF-CC1-PS3	63	1	0	1.0E-7	1.0E-1
RF-CC1-H2O	62	1	0	1.0E-7	1.0E-1
RF-CC2-SYN	73	1	0	1.0E-7	1.0E-1
RF-CC2-1AP	69	1	0	1.0E-7	1.0E-1
RF-CC2-FAP	72	1	0	6.0E-3	5.0E-1
RF-CC2-ANT	65	1	0	1.0E-7	1.0E-1
RF-CC2-MCP	66	1	0	1.0E-7	1.0E-1
RF-CC2-HVF	67	1	0	1.0E-7	1.0E-1
RF-CC2-PS1	68	1	0	1.0E-7	1.0E-1
RF-CC2-PS2	71	1	0	1.0E-7	1.0E-1
RF-CC2-H2O	70	1	0	1.0E-7	1.0E-1

Table 4-1. (continued)

Component ID	ID number in tree	Number in units	Redundancy	λ (1/hr)	μ (1/hr)
RF-EC1-OST	91	1	0	3.0E-3	2.5E-1
RF-EC1-PWS	90	1	0	1.4E-3	4.0E-2
RF-EC1-ANT	86	1	0	1.0E-7	1.0E-1
RF-EC1-MCP	87	1	0	1.0E-7	1.0E-1
RF-EC1-HVF	88	1	0	1.0E-7	1.0E-1
RF-EC1-H2O	89	1	0	1.0E-7	1.0E-1
RF-EC2-OST	97	1	0	3.0E-3	2.5E-1
RF-EC2-PWS	96	1	0	1.4E-3	4.0E-2
RF-EC2-ANT	92	1	0	1.0E-7	1.0E-1
RF-EC2-MCP	93	1	0	1.0E-7	1.0E-1
RF-EC2-HVF	94	1	0	1.0E-7	1.0E-1
RF-EC2-H2O	95	1	0	1.0E-7	1.0E-1
RF-EC3-OST	79	1	0	3.0E-3	2.5E-1
RF-EC3-PWS	78	1	0	1.4E-3	4.0E-2
RF-EC3-ANT	74	1	0	1.0E-7	1.0E-1
RF-EC3-MCP	75	1	0	1.0E-7	1.0E-1
RF-EC3-HVF	76	1	0	1.0E-7	1.0E-1
RF-EC3-H2O	77	1	0	1.0E-7	1.0E-1
RF-EC4-OST	85	1	0	3.0E-3	2.5E-1
RF-EC4-PWS	84	1	0	1.4E-3	4.0E-2
RF-EC4-ANT	80	1	0	1.0E-7	1.0E-1
RF-EC4-MCP	81	1	0	1.0E-7	1.0E-1
RF-EC4-HVF	82	1	0	1.0E-7	1.0E-1
RF-EC4-H2O	83	1	0	1.0E-7	1.0E-1
PP-ECH	98	1	0	1.0E-7	1.0E-1
PP-GPS	99	1	0	1.0E-7	1.0E-1
PP-GAS	100	1	0	1.0E-7	1.0E-1
DS-MII	119	18	0	2.2E-3	4.0E-1
DS-DIL	101	7	0	1.0E-7	1.0E-1
DS-CEA	102	1	0	2.3E-4	2.1E-2
DS-TOF	103	1	0	1.0E-7	1.0E-1
DS-TSS	104	1	0	1.0E-7	1.0E-1
DS-GEL	107	2	0	1.0E-7	1.0E-1
DS-GEA	109	1	0	1.0E-7	1.0E-1
DS-LPS	105	8	0	1.0E-7	1.0E-1
DS-LPD	106	2	0	1.0E-7	1.0E-1
DS-SEP	108	1	0	1.0E-7	1.0E-1

Table 4-1. (continued)

Component ID	ID number in tree	Number in units	Redundancy	λ (1/hr)	μ (1/hr)
DC-CAM1	110	1	0	2.3E-4	2.8E-3
DC-CAM2	112	1	0	2.3E-4	2.8E-3
DC-MVA1	111	1	0	1.0E-7	1.0E-1
DC-MVA2	113	1	0	1.0E-7	1.0E-1
DC-VAX	114	1	0	1.0E-7	1.0E-1
DC-ETH	115	1	0	1.0E-7	1.0E-1
DC-GRD	116	1	0	2.3E-4	2.0E-0
OP	117	1	0	1.0E-7	1.0E-1

Table 4-2. Availability and Importances

System ID	Availability %	Importance BIRNBAUM	CRITICALITY
MC-FS1	100.0	0.571	1.0
MC-FS2	100.0	0.571	1.0
MC-TR1	100.0	0.571	1.0
MC-TR2	100.0	0.571	1.0
MC-TR3	100.0	0.571	1.0
MC-TR4	100.0	0.571	1.0
MC-CB1	100.0	0.571	1.0
MC-CB2	100.0	0.571	1.0
MC-CB3	98.0	0.583	1.0
MC-ERB	100.0	0.571	1.0
MC-MGE	100.0	0.571	1.0
MC-PS1	100.0	0.571	1.0
MC-PS2	100.0	0.571	1.0
MC-PS3	100.0	0.571	1.0
MC-PS4	100.0	0.571	1.0
MC-PH1	99.7	0.573	1.0
MC-PH2	99.7	0.573	1.0
MC-PH3	99.7	0.573	1.0
MC-TM1	99.9	0.571	1.0
MC-TM2	99.9	0.571	1.0
MC-TM3	99.9	0.571	1.0
MC-SC1	99.9	3.43	6.0
MC-SC2	99.9	3.43	6.0
MC-SC3	99.9	3.43	6.0
MC-SC4	99.9	3.43	6.0
MC-SC5	99.9	3.43	6.0
MC-SC6	99.9	3.43	6.0
MC-SC7	99.9	3.43	6.0
MC-CCC	100.0	4.57	8.0
MC-SCA	99.7	1.15	2.0
MC-MSC	99.7	2.29	4.0
MC-CHC	100.0	1.14	2.0
MC-SCB	99.7	3.44	6.0
MC-COL	100.0	1.14	2.0
MC-IF1	99.7	0.573	1.0
MC-IF2	99.7	0.573	1.0
WS-CWS	100.0	0.571	1.0
WS-DIS	100.0	0.571	1.0
WS-PMP	100.0	0.571	1.0
WS-PIP	100.0	0.571	1.0
WS-VLV	100.0	0.571	1.0

Table 4-2. (continued)

System ID	Availability %	Importance BIRNBAUM	Importance CRITICALITY
VS-VCV	99.1	0.576	1.0
VS-RP5	100.0	0.571	1.0
VS-RP1	100.0	0.571	1.0
VS-RP2	100.0	0.571	1.0
VS-RP3	100.0	0.571	1.0
VS-RP4	100.0	0.571	1.0
VS-CP1	99.6	2.23E-3	3.89E-3
VS-CP2	99.6	2.23E-3	3.89E-3
VS-TP1	100.0	4.86E-5	8.51E-5
VS-TP2	100.0	4.86E-5	8.51E-5
VS-MGV	100.0	0.571	1.0
VS-NV1	99.99	2.22E-3	3.89E-3
VS-NV2	99.99	2.22E-3	3.89E-3
VS-NV3	99.99	4.86E-5	8.51E-5
VS-NV4	99.99	4.86E-5	8.51E-5
VS-TSB	99.6	0.597	1.0
VS-IOG	99.99	0.571	1.0
VS-CTL	100.0	0.571	1.0
VS-WT1	100.0	0.571	1.0
VS-WT2	100.0	0.571	1.0
VS-WT3	100.0	0.571	1.0
VS-WT4	100.0	0.571	1.0
RF-CC1-SYN	100.0	0.571	1.0
RF-CC1-1AP	100.0	0.571	1.0
RF-CC1-2AP	99.9	0.572	1.0
RF-CC1-FAP	98.9	0.578	1.0
RF-CC1-ANT	100.0	0.571	1.0
RF-CC1-MCP	100.0	0.571	1.0
RF-CC1-HVF	100.0	0.571	1.0
RF-CC1-PS1	100.0	0.571	1.0
RF-CC1-PS2	100.0	0.571	1.0
RF-CC1-PS3	100.0	0.571	1.0
RF-CC1-H2O	100.0	0.571	1.0
RF-CC2-SYN	100.0	0.571	1.0
RF-CC2-1AP	100.0	0.571	1.0
RF-CC2-FAP	98.8	0.578	1.0
RF-CC2-ANT	100.0	0.571	1.0
RF-CC2-MCP	100.0	0.571	1.0
RF-CC2-HVF	100.0	0.571	1.0
RF-CC2-PS1	100.0	0.571	1.0
RF-CC2-PS2	100.0	0.571	1.0
RF-CC2-H2O	100.0	0.571	1.0
RF-EC1-OST	98.8	0.578	1.0
RF-EC1-PWS	96.6	0.591	1.0
RF-EC1-ANT	100.0	0.571	1.0

Table 4-2. (continued)

System ID	Availability %	Importance BIRNBAUM	Importance CRITICALITY
RF-EC1-MCP	100.0	0.571	1.0
RF-EC1-HVF	100.0	0.571	1.0
RF-EC1-H2O	100.0	0.571	1.0
RF-EC2-OST	98.8	0.578	1.0
RF-EC2-PWS	96.6	0.591	1.0
RF-EC2-ANT	100.0	0.571	1.0
RF-EC2-MCP	100.0	0.571	1.0
RF-EC2-HVF	100.0	0.571	1.0
RF-EC2-H2O	100.0	0.571	1.0
RF-EC3-OST	98.8	0.578	1.0
RF-EC3-PWS	96.6	0.591	1.0
RF-EC3-ANT	100.0	0.571	1.0
RF-EC3-MCP	100.0	0.571	1.0
RF-EC3-HVF	100.0	0.571	1.0
RF-EC3-H2O	100.0	0.571	1.0
RF-EC4-OST	98.8	0.578	1.0
RF-EC4-PWS	96.6	0.591	1.0
RF-EC4-ANT	100.0	0.571	1.0
RF-EC4-MCP	100.0	0.571	1.0
RF-EC4-HVF	100.0	0.571	1.0
RF-EC4-H2O	100.0	0.571	1.0
PP-ECH	100.0	0.571	1.0
PP-GPS	100.0	0.571	1.0
PP-GAS	100.0	0.571	1.0
DS-MII	99.5	10.3	18.0
DS-DIL	100.0	4.00	7.0
DS-CEA	98.9	0.577	1.0
DS-TOF	100.0	0.571	1.0
DS-TSS	100.0	0.571	1.0
DS-GEL	100.0	1.14	2.0
DS-GEA	100.0	0.571	1.0
DS-LPS	100.0	4.57	8.0
DS-LPD	100.0	1.14	2.0
DS-SEP	100.0	0.571	1.0
DC-CAM1	92.4	0.618	1.0
DC-CAM2	92.4	0.618	1.0
DC-MVA1	100.0	0.571	1.0
DC-MVA2	100.0	0.571	1.0
DC-VAX	100.0	0.571	1.0
DC-ETH	100.0	0.571	1.0
DC-GRD	99.9	0.571	1.0
OP	100.0	0.571	1.0

Table 4-3. System/Subsystem Availability

System ID	Availability
MC	93.3
WS	100.0
VS	98.7
RF	81.0
PP	100.0
DS	90.6
DC	85.4
Phaedrus	57.1

(ii) An unavailability driver is the RF system. Phaedrus availability could significantly increase if the arcing problems are solved.

(iii) The diagnostics system, in particular, the microwave interferometer, can be an unreliabiity driver because of the large number of identical units without redundancy.

Recall the actual success ratio is about 99% for 268 successive shots as shown in Section 3.3. The value would not vary much for different series of experiments. Thus the availability of Phaedrus is very high at least from the experimentalist's point of view. This seems to contradict the estimated availability that is less than 60%. Although detailed analysis for this discrepancy is beyond the scope of the present report and it will be investigated in the future, we give a brief discussion as follows:

* The MTTFs and MTTRs used in the analysis are not statistical averages. As more date is collected, these values may change considerably.

* The success ratio of the shots calculated from the operation records is not equivalent to the availability which is defined as the uptime divided by the total operation time. If a subsystem fails and it is repaired by stopping experiments, then there are no shots made during the repair. The down time is not reflected in the success ratio. Thus we apparently overestimate the availability.
* We estimated a steady-state availability. However, the steady-state assumption is not correct because a series of experiments which last a few days is usually preceded by intensive testing and preventive maintenance. Thus it may be better to assume a system as good as new at the beginning of an experiment. With this assumption the reliability is calculated. We use the systems tree given in Fig. 4-1 and the MTTFs given in Table 4-1 (MTTFs for components which have never failed or have no data available are set to 1.0E-27). The reliability at one day after an experiment is initiated is 16%.

5. CONCLUSIONS AND FUTURE DIRECTTIONS

A reliability analysis of the tandem mirror Phaedrus has been performed. Some suggestions are made to improve the reliablity. A data management computer system CREDO has been adapted for data collection on-site. The present study is the first of a series of studies. We will establish a data collection methodology based on the CREDO system at the Phaedrus facility. The method can be used at any small lab around the world. The collected data must be statistically processed and analyzed. We will develop computer programs for that. Finally the data can be stored in the FUSEDATA system for use by fusion reactor designers. The operation logs must be modified so that we can see the precise operational history; we need the length of down time and its cause (preventive/corrective maintenance or testing) and the state of discharges (success or failure judged by experimentalists).

ACKNOWLEDGEMENTS

This work was performed under the auspices of the Office of Magnetic Fusion of U.S. Department of Energy. I am grateful to Drs. Hershkowitz, Breun, Ferron, Majeski, Mr. Pew, and Mr. Brooker. I appreciate Ms. Gruetzmacher for providing and modifying her computer program.

REFERENCES

1. Z. Musicki and C.W. Maynard, "The Availability Analysis of Fusion Power Plants as Applied to MARS," Nuclear Technology/Fusion 4, 284-289 (1983).

2. R. Bunde, "Availability Assurance of NET-Strategy and Status of Work," EUR XII324/33, NET/IN/84-074, EUX, 1985.

3. B.J. Green, R. Saunders and D. Webberley, "Summary of 1985 Operation Week 2-24," Joint European Torus report JET-IR(86)02, (1986).

4. R.A. Camp, "TFTR System Availability Analysis and Growth Methodologies," Proc. 11th Symp. on Fusion Engineering, pp. 209-210, Nov. 18-22, 1985, Austin, TX, 1985.

5. R.F. Parsells and H.P. Howard, "Application of Quality Requirements in Fusion Research," ibid., pp. 327-329.

6. R.R. Lauze, P.G. Karsner and J.W. Heefner, "Quality Assurance for Electron Cyclotron Resonance Heating (ECRH)," ibid., pp. 209-210.

7. N. Ogiwara, T. Arai and M. Shimizu, "Reliability Tests of 40 cm ID Cell Metal Gate Valve and 54 cm ID Ceramic Break for JT-60," Proc. 10th Symp. on Fusion Technology, pp. 1058-1062, Philadelphia, PA, Dec. 5-9, 1983.

8. I. Kondo et al., "Reliability Aspects in the JT-60 Central Control System Design," ibid., pp.1933-1936.

9. K. Kurihara et al., "System Design for JT-60 Failure Mode Analysis and Prediction," ibid., pp. 1954-1958.

10. J.B. Czirr, T. Thome and R.W. McNamara, "Large Coil Test Facility Fault Tree Analysis," Minority Enterprise Service Assoicates, Orem, UT (August 1983).

11. O. Vollmer, "Availability of Neutral Beam Injection," NET report EUR-FU/XII-361/85/49 (1985).

12. H. Schnauder and A. Wickenhauser, "Reliability of a Current Switch Down in a Neutral Beam Injector in Case of a Plasma Disruption," Kernforschungszentrum Karlsruhe GmbH, May 1985.

13. R.V. Carlson, S.P. Cole, F.A. Damiano and W.A. Stone, "Early Operating Experience with the Tritium Systems Test Assembly Tritium Waste Treatment System," Proc. 2nd National Topical Meeting on Tritium Technology in Fission, Fusion and Isotope Applications, Dayton, Ohio (April 1985).

14. S.L. Thomson, A. Dabiri, D.C. Keeton, B.W. Riemer and L.M. Wagner, "Availability Program Phase I Report," ORNL/FEDC-84/10 (May 1985).

15. Z. Musicki and C.W. Maynard, "AVSYS, A Computer Program for Fusion Availability Calculations," University of Wisconsin Fusion Technology Institute Report UWFDM-531 (Jan. 1984).

16. Y. Watanabe, "PROPA: Probabilistic Performance Analysis Program," University of Wisconsin Fusion Technology Institute Report UWFDM-657 (Nov. 1985).

17. Y. Watanabe, "Symbolic Manipulation of Structure Functions in Availability Analysis," University of Wisconsin Fusion Technology Institute Report UWFDM-658 (Nov. 1985, revised Nov. 1986).

18. A. Bennethum et al., "FUSEDATA - A Fusion Systems Data Base," University of Wisconsin Fusion Technology Institute Report UWFDM-673 (July 1986).

19. K.M. Gruetzmacher, "Failure/Maintenance Data Base for the Tritium Systems Test Assembly," University of Wisconsin Fusion Technology Institute Report UWFDM-653 (Dec. 1985).

20. R. Breun et al., "Initial Results from the Tandem Mirror Phaedrus," in Plasma Physics and Controlled Nuclear Fusion Research (Proc. 8th Int. Conf., Brussels, 1980), Vol. 1, p. 105, IAEA, Vienna (1981).

21. N. Hershkowitz et al., "Plasma Potential Control and MHD Stability Experiments in the Phaedrus Tandem Mirror," in Plasma Physics and Controlled Nuclear Fusion Research (Proc. 10th Int. Conf., London, 1984), Vol. 2, p. 265, IAEA, Vienna (1985).

22. N. Hershkowitz, "RF Heating in Tandem Mirrors," International School of Plasma Physics, Monotypia Franchi, Citta di Castell (Perugia) Italy (1984).

23. G.V. James, "Water Treatment," 4th ed., Technical Press (1971).

24. A. Roth, "Vacuum Technology," 2nd ed., North-Holland Pub. Co., Amsterdam (1982).

25. IEEE, CAMAC Instrumentation and Interface Standards, New York, IEEE press (1982).